D6.3 Li-ion battery pretreatment process assessment

Project	Green Transport Delta - Electrification
Project number	MOB21011
Author(s)	Cody van Beek-Hagemans, Eda Yilmaz, Susanne van Berkum, Emma Folkertsma
Version	3.0
Date	5 September 2024

Revision index

Version	Description	Date
3.0	Final version	05-09-2024
2.0	Feedback review processed	02-09-2024
1.0	Draft for review technical coordinator and TNO internal review	26-07-2024

Contact details

Name	Role	Email
Dr. Susanne van Berkum	Consultant	susanne.vanberkum@tno.nl
Dr. Cody van Beek-Hagemans	Scientist	cody.vanbeek@tno.nl
Dr. Eda Yilmaz	Scientist	eda.yilmaz@tno.nl
Dr. Emma Folkertsma	Project manager and work package 6 lead	emma.folkertsma@tno.nl

Inhoud

1.   Summary

Lithium ion batteries contain many critical raw materials (e.g. Ni, Mn, Co, and Li) and end-of-life batteries are available and collected in the Netherlands. However, an infrastructure to recycle these is not here yet in place. Due to geopolitical tensions regarding the supply of critical raw materials and EU's battery regulations, the development of a battery recycling infrastructure in the EU is needed with a specific role for the Netherlands. Battery recycling often involves a pretreatment process, followed by chemical processing to recover the (critical) metals. The pretreatment process involves multiple steps, among which are shredding and sieving, and results in the formation of a fine powder fraction, called black mass, which is enriched in these critical metals and graphite. In the Netherlands, an innovative pretreatment process is in development at pilot scale. This process is suitable for processing charged batteries by shredding them under inert atmosphere circumventing the need of a discharging step and simultaneously being able to usefully apply the released energy.

This work focusses on the assessment and optimisation of this pretreatment process. The process assessment is done by determining 1) the black mass recovery efficiency by setting up a mass balance for the process, 2) the quality of the output materials by looking at its chemical and physical composition, 3) efficiency of the removal of the electrolyte by looking at the mass balance and analysing various output streams, 4) the impact of the partial pyrolysis due to shredding of charged batteries on quality of output materials by varying the charging state of the input materials. Additionally, the ability to increase the recovery of cathode active materials was studied by testing several extra processing steps for the residual fraction. To do this, multiple battery shredding trials were performed with different feedstock parameters to explore the influence of varying input materials. In particular, the influence of the state of charge, the battery chemistry, and the presence of casing on the pretreatment process and resulting output materials were examined. In addition, material emissions during the processing were measured, and included in the mass balance.

The main findings from this study are that for the battery shredding trials performed (with either NMC, NCA or LFP battery chemistry with varying state of charge), a mass balance could be made that would add up to 97-99% of the input weight. Loss of mass is partly explained by the formation of gaseous products like CO_2 and water vapor that are formed by thermal decomposition and burning of the organic components/solvents in the batteries. During the battery shredding trials, the collected condensate was analysed, showing the presence of some of the battery electrolyte solvents, water, and (one of) the main components, dimethyl carbonate, was quantified. Furthermore, it was shown that the particulate matter emitted during the trials, containing both graphite and cathode active materials, did not play a significant role in the gap in the mass balance.

The electrolyte removal was efficient in the case of batteries with NMC and NCA chemistry, but still about 1-2 wt% of electrolyte solvents was present in the black mass fraction. A higher percentage of remaining electrolyte solvents (~5%) was present in the black mass fraction of LFP batteries. The composition of these solvents in the black mass and condensate fractions had a different composition compared to the NMC and NCA batteries containing more solvents with a higher boiling point. Large LFP batteries with a mass of 2 kg, which therefore contain a larger amount of electrolyte solvents compared to smaller batteries (<100 g each), were hard to handle by the current operating conditions. This resulted in a less efficient separation of the fine powder of the black mass from the coarse fraction for these LFP batteries, as is evidenced by the mass balance and elemental analysis of both the black mass fraction and the coarse fraction. The cathode active material content in the black mass and coarse fractions of all battery shredding trials was quantified. Interestingly, it was observed that for the NMC

and NCA batteries more than 50% of the cathode active material remains in the coarse fraction and for the LFP batteries this is more than 75%. This shows that the separation of the black mass from the coarse material is not optimal and results in significant amount of desired cathode active material remaining trapped in the coarse fraction. This could be due to too short residence time and inefficient shaking in the sieving table, the presence of electrolyte solvents which make the cathode active material particles stick more to the coarse particles, and a suboptimal sieving system, since the sieving diameter used is rather large compared to the average particle size in the black mass powder, as was shown by SEM analysis.

To understand the (chemical) composition of the black mass, condensed liquid fraction, and the coarse fraction better, various analytical techniques were employed which showed which materials of a battery end up in which fraction. One of the key findings is that graphite, plastic, binder, current collectors, cathode active material, and some electrolyte solvents all (partly) end up in the black mass fraction, indicating that the black mass fraction is a complex mixture of different materials. This is similar for the coarse fraction, showing that graphite and cathode active materials remain trapped in this fraction.

Having established that significant amounts of cathode active materials are trapped still in the coarse fraction after the pretreatment process, various methods were employed to recover the black mass from the coarse particle stream. With an emphasis on the coarse material from the NMC trial, it was shown how effective various methods were to recover the cathode active materials from the coarse fraction. Based on ICP-MS analysis and determining the elemental composition of the coarse fraction before and after the various treatments, showed that after an additional processing step, still more than half of the cathode active materials remain in the coarse fraction and optimization of these methods is required to collect as much cathode active material from the end-of-life batteries as possible.

2.   Introduction

Challenge

The rise in the number of electric vehicles in the Netherlands results in a growing quantity number of lithium ion batteries present in the Netherlands and the collection of spent batteries is well-organized. However, the recycling of lithium ion batteries takes place abroad, resulting in the export of the resulting materials. Changes in the geopolitical landscape makes it even more important to get a hold on resources to maintain and strengthen our trading position. Geological mines are not available in Netherlands, but the urban mine offers unique opportunities: the urban mine refers to the stockpile of urban waste and is a highly valuable secondary source of resources that should be optimally utilized. Recovering critical materials from batteries is also an important consideration in the EU level. The new EU battery regulation, that have become effective in 2023, set very high demands on the recycling of (lithium ion) batteries and recovery of the metals present in these batteries: 95% of the cobalt and nickel and 80% of lithium have to be recovered by 2032 (Parliament, 2023).

The current processing of spent batteries takes place in two steps: first a pretreatment process to liberate to separate the cathode and anode active materials from casing and current collector foils and next a chemical processing to separate and recover the (critical) materials as secondary raw materials. Both steps have seen lots of developments already but are not yet fit for the future: they do not fulfill the high demands of the EU battery regulations (Parliament, 2023). The pretreatment typically involves the following steps: discharging, dismantling, comminution, and sorting, which finally results in a fine, black powder called black mass (see report GTD-E project task 6.1). The black mass is the fraction that is concentrated in the cathode and anode materials, which contain many of the critical and valuable materials within a battery, such as cobalt, nickel, and lithium (cathode) and graphite (anode). This material stream is then chemically processed to recover the valuable metals.

Literature reports concerning pretreatment processes show that these steps result in significant material losses (Kim et al., 2021): only 75 – 90% of the cathode materials that enter the process will end up in the black mass fraction (Latini et al., 2022). It is likely that some of the valuable cathode active material (CAM) is lost in residual fractions of preprocessing steps. This offers the opportunity to increase the percentage of CAM that can be recovered. Another challenge in the pretreatment process is the need for deep discharging the batteries prior to dismantling and comminution can take place safely. Multiple discharging methods exist, but these all require additional infrastructure, take time, and are costly. It would be desired if a pretreatment process is developed that can perform all common pretreatment steps without the need for deep discharging.

Solution

A Dutch company, Future Recycling Technologies (FRT), aims to improve the pretreatment of end-of-life batteries and has developed a new technology that does not require the prior deep discharging of batteries. By controlling the supply of batteries to their system and by working under inert atmosphere the batteries containing residual energy are comminuted. Ideally, the residual energy is put to use: during comminution of the batteries, the residual electrical energy is converted to heat, which enables the separation of the liquid electrolyte from the solid materials by evaporation. Separation of the liquid electrolyte from the solids has the advantage that it is no longer a contaminant in the chemical separation step of black mass. This pretreatment process can have considerable advantages: the residual energy

is put to good use, investments in costly deep discharging equipment are prevented, but also the time-consuming deep discharging step is prevented.

Currently, this technology is being tested on a pilot scale and is still being optimized. At the moment, FRT is the only party in the Netherlands that is making tangible steps to start up the battery recycling chain in the field of pretreatment. This is why their process is selected for performing the preprocessing trials in the Green Transport Delta – Electrification project.

The first activity within task 6.3 focusses on the assessment of the efficiency of the liquid electrolyte removal in the process and the impact on the separation of black mass from the other materials. This will be done by determining a full mass balance in which all input and output materials are taken into account. The second activity is to investigate the composition of the material output streams. A third activity is to study the CAM recovery and investigate how much CAM ends up in the fine black mass fraction and other output streams by quantification of these elements in the various streams. A full (material) analysis of the black mass fraction and the other fractions will provide insight into the amount and composition of CAM in the output material streams. This allows to determine and quantify the losses of CAM in other output streams in the current pretreatment process. A fourth activity is the study and collection of emissions of volatile organic compounds and particulate matter by air sampling and measurements to determine the loss of mass. The last activity is to employ various processes to recover CAM from the coarse material stream.

To summarize, the research questions to be answered by the activities in this task are the following:
-     To what extent is the liquid electrolyte removed from the solids by the process?
-     How much of the CAM is currently recovered as black mass in this pretreatment process?

A flexible pretreatment process can process many different types of batteries with different battery chemistries, cell sizes and types and casings with different states of charge. Therefore, the influence of a selection of these parameters on the mass balance, and output materials will be studied. In particular, the influence of different battery chemistries (NMC, NCA, or LFP), presence of battery casing and battery state of charge will be examined.

3.   Pretreatment setup and analysis plan

The pretreatment setup operates on a pilot scale (50 kg/h scale) and is able to process different types of end-of-life battery feeds without any deep discharging steps. The process results in three collected product streams: a fine powder (black mass), a coarse particle, and a condensate fraction. The electrolyte solvents and other volatile products are expected to end up in the condensate. In addition, non-condensable volatile products will be adsorbed on activated carbon filters. This chapter describes how the trials have been performed and which different types of battery feeds are shredded.

3.1   Pretreatment installation

The pilot-scale battery pretreatment setup is shown in Figure 1, which displays the six different compartments A-F of the setup: (A) the inlet, (B) the shredder, (C) the sieving table and (D) the outlet, (E) the condenser and (F) the activated carbon filters.

Figure 1: Image of the battery pretreatment setup with the battery inlet (A), battery shredder (B), sieving table (C) and solid fraction collection (D), condenser (E, on the back of the setup), and activated carbon filters (F) indicated.

On the top of the setup, the battery inlet of compartment A is present. Below the inlet, comminution is performed by the battery shredder, under inert conditions, in compartment B. During shredding, energy is released due to short-circuiting of the cells. The released energy heats the shredded material, enabling evaporation of the electrolyte solvents and other volatile components. Compartment C is the sieving table underneath the battery shredder. The main function of compartment C is separation of the coarse particle fraction from the fine fraction (black mass). The temperature in compartment C is maintained at elevated temperature by additional heating in order to support the evaporation of the

volatile electrolyte solvents. The vapours of the electrolyte solvents are passed over a condenser, which condenses volatile products that are formed and released during the shredding process. After the condenser, the atmosphere is passed over an activated carbon filter unit to adsorb any residual volatile organic components and adsorb hydrogen fluoride (HF) and other toxic fluorine containing compounds that may be formed in the shredding process. The activated carbon filter is impregnated with base to be able to adsorb HF and similar toxic compounds well. After the sieving table, the solid particle streams are collected in two separate collection bags. The whole setup operates under an inert atmosphere. In addition, the battery inlet and product outlets are protected from the ambient atmosphere by valved loading chambers.

3.2   Trials performed with the pretreatment process

Feedstock

Six different trials with various battery chemistries, state of charge and presence of casing were performed (see Table 1).

Table 1: Overview of the different trials performed and the parameters that were changed.

Trial no.	Battery Chemistry	State of Charge	Voltage range (average)	In casing or dismantled
1	NMC	Low	0.0 – 18.0 V (15.8 V)	Casing
2[a]	NMC	High	18.6 – 20.3 V (19.9 V)	Casing
3	NCA	High	3.6 V	Dismantled
4	NCA	Low	n.a.	Dismantled
5	LFP	Low	n.a.	Dismantled
6	LFP	High	n.a.	Dismantled

[a] An additional batch of NMC batteries with unknown state of charge was shredded prior to trial 2, which was followed by shaking and emptying the setup output streams prior to the batch of trial 2.

The three different battery chemistry types used for the trials, are so called NMC (lithium nickel manganese cobalt oxides), NCA (lithium nickel cobalt aluminium oxides), and LFP (lithium iron phosphate), see Figure 2. These materials are used as CAM within battery cells. The setup output materials were emptied between different batches and the trial number is based on the chronological order when these trials were performed.

Figure 2: Different battery types that were used for the different trials with NMC batteries in casing (left), cylindric NCA cells (middle), and large prismatic LFP cells (right).

In addition, the trials involved battery cells in casing (trials 1 and 2) and without casing (trials 3-6) and different State of Charge (SoC): high SoC (trial 1, 4, 5) and low SoC (2, 5, 6). The exact SoC could not be determined, therefore, the voltage of the battery cells or batteries was measured to get an indication of the SoC meaning a relatively low voltage would correspond to low SoC and a relatively high voltage would correspond to high SoC. These changing parameters can give insights into how the SoC, presence of cell casing, and battery chemistry affects the output material streams and efficiency of electrolyte and black mass separation.

Monitoring

During all shredding trials, the following parameters were monitored and registered:
- the temperature of the shredder (B);
- the temperature of the sieving table (C);
- CO_2 level (% of atmosphere in installation) (B);
- O_2 level (% of atmosphere in installation) (B);
- Occurrence of an exothermic discharge and other observations.

The O_2 level in the set up was monitored closely to ensure safe shredding and was kept under 8 %. The CO_2 level was registered to monitor any discharges following shredding of batteries.

For the first two trials (NMC), emissions from the set up were measured. Figure 3 shows a schematic representation: emissions of particles (using air filters and stubs, represented by the filled bubbles and bucket and sweep icons respectively) and volatile organic compounds (using cannisters represented by the open bubbles) were sampled and real-time monitored at three different locations around the pretreatment setup.
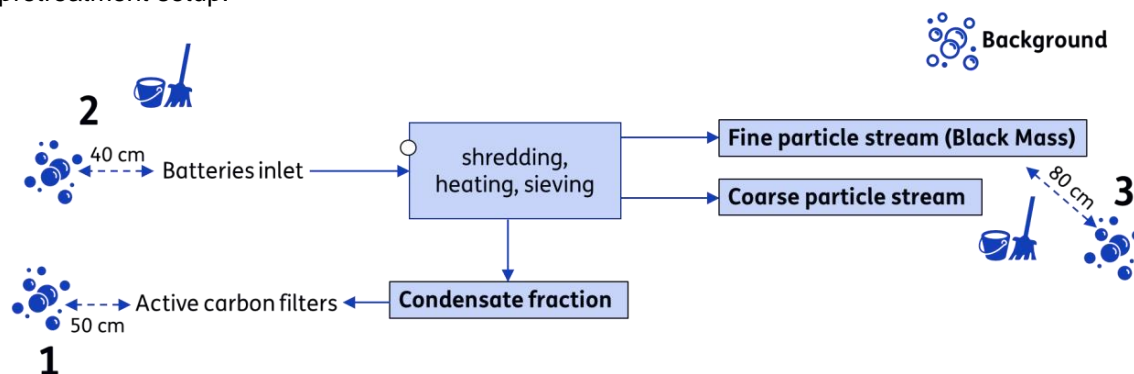

Figure 3: Schematic representation of the battery pretreatment setup and material fractions collected with the location of the three measurement setups 1, 2, and 3 indicated.

Description of NMC trials

The batteries used for the NMC trials involved Parkside power tools (20 V, 2 Ah) containing cylindrical NMC battery cells as shown in Figure 4. During trial 1 charged batteries with measured average voltage of 19.86 V (range 18.55 – 20.30 V) were treated. In trials 2 low charge batteries were shredded with an average voltage of 15.82 V (range 0.00 – 18.00 V). charge. The batteries with unknown charge are not further discussed.

Figure 4: One of the battery packs used in the first two trials containing NMC battery cells.

Figure 5: The mass of the NMC battery packs (left), the individual NMC battery cells within one pack (middle), and the mass of the battery management system within one battery pack (right).

The battery packs used in trial 1 and 2 weigh approximately 430 g. Such pack contain five cylindrical NMC cells as well as a printed circuit board that is part of the battery management system. The casing is made of polymeric material as well as glass fibre as denoted on the casing (polyamide). Therefore, the output materials will contain plastics (e.g. nylon/polyamide, polypropylene, polyethylene) and various metals and glass fibre (printed circuit board and casing), which would not be present in trials involving only battery cells. The larger heterogeneity and higher complexity of these additional materials could influence the shredding process and the electrolyte and black mass separation steps.

In the first trial, a total of 17 battery packs (low SoC NMC cells) were shredded, with a new battery pack added after every one minute. Initially, the temperature of the shredder was 20 °C, which slowly heated up during the trial to 23 °C. The sieving table was at a low initial temperature of 43 °C when the first battery was shredded and was in three minutes heated to 79 °C. During the course of shredding the uncharged battery packs, the sieving table temperature fluctuated between 70-76 °C. The CO_2 concentration remained rather stable during this trial and was between 9.4 and 10.4%. However, the oxygen concentration varied more. At the start of the trial, the concentration was 4.5%, but it increased over time to 6-7%. With these uncharged battery packs, no exothermic discharges were observed. After the last battery pack was shredded, the setup was operated for another 10 minutes to obtain most of the solid and liquid product.

Between the first and second trial another batch of 21 batteries was shredded. These battery packs had an unknown SoC and the output materials were not analysed. However, the output materials were taken into account for the mass balance of the first two trials.

During trial 2, a total of 20 NMC-chemistry battery packs with a high SoC ere shredded. Just after the first battery pack was added, the shredder was at a temperature of 29 °C, the sieving table at 78 °C, CO_2 at 9.2% and oxygen at 5.9%. Every minute, a battery pack was added. After the third battery pack, the sieving table was 79 °C and the oxygen concentration dropped to 4.2%. During the trial, the temperature of the shredder slowly increased to 34 °C and the temperature of the sieving table remained rather stable between 74-81 °C. The CO_2 concentration remained around 9% for the first 14 battery packs and the oxygen concentration was between 5-6.6%. In general, no exothermic discharges were, however, during shredding of one of the battery packs, an exothermic reaction was observed, leading to an increase of the CO_2 concentration to 11.5% and a significant decrease of the oxygen concentration to 3% which slowly increased to 5.5% with the remaining battery packs. After the 17th battery pack, fumes were observed from the battery inlet as well as at the outlet of the activated carbon filters. To determine what compounds were emitted in the fumes, an additional cannister was used to sample the atmosphere. After all battery packs were added, the setup was operated for another half an hour to collect most of the materials (total operation time ~1h). Afterwards, all solid outputs and the condensate were collected. When calculating the mass balance, a significant quantity of mass appeared to be missing. For that reason, the set up was operated again for a longer time by using the sieving table to obtain as much as material as possible. This quantity is referred to as extra solid fraction in Figure 8.

For these first two trials, also different filters as well as cannisters were placed at measuring points 1, 2 and 3 (Figure 3) to collect emissions. The collected material on these filters was then analysed using various analytical techniques to determine the mass, composition and morphology of the particulate matter emitted during operation of the setup and compared to background particulate matter. In addition, ultrafine particle (UFP) (nanosized particulate matter), emissions were monitored during the trials, and the monitors indicated that there was a high emission of UFP during the trials.

Description of NCA trials

The third and fourth trial involved cylindric NCA battery cells without casing. In trial 3 high charge battery cells were shredded and in trial 4 the battery cells had a low SoC. The battery cells that were used for these two trials are shown in Figure 6.

Figure 6: The NCA battery cells that were used for trials 3 and 4.

Each NCA battery cell weighs approximately 47.2 g. Typically, six batteries were fed to the set up simultaneously. The output material from these trials is expected to be less heterogeneous and would contain much less plastic and complexity due to the absence of casing and battery management system compared to trials 1 and 2.

In trial 3, a total of 156 NCA battery cells with a high SoC were added in a total of 26 battery feeds of six battery cells each feed. The cells were added every two minutes apart. The pretreatment setup was slightly modified between trials 1 – 2 and 3 - 6 in such a way that the sieving table was better insulated to keep the heat inside and the condenser was modified to improve electrolyte removal. At the start of the trial the temperature of the shredder was 19 °C, which slowly heated up to 35 °C over time. The temperature of the sieving table started at 88 °C and increased to 115 °C after the first 12 battery feeds, after which the active heating of the sieving table was turned off. This made the temperature of the sieving table go down to about 90 °C during the remainder of the trial. The CO_2 concentration during this trial was considerably higher compared to trial 4 (see below) and was generally found between 11 and 15%. The oxygen concentration fluctuated around 4-5% during the trial. In 15 of 26 battery feeds, an exothermic discharge was observed. In 4 of 26 battery feeds, the activated carbon filters were fuming and two times a loud bang was heard during the shredding. After the last battery feed, the setup was operated for another 15 minutes to obtain most of the product.

For trial 4, a total of 160 NCA battery cells with a low SoC were shredded in 22 separate batches. Battery cells were added every two minutes apart. At the start of the trial, the temperature of the shredder was 26 °C, which over the course of the trial heated up to 36 °C. The temperature of the sieving table was higher compared to trials 1 and 2 and started at 94 °C. The temperature of the sieving table was generally between 87 and 96 °C. After shredding the first battery cells, the CO_2 concentration was 8.3%, which during the trial would increase to 10-11%. The concentration of oxygen started out at 6.3% and increased to 8.8% the first 10 minutes, but after that it decreased quickly to about 4% for the remaining time of the trial. The optimum number of battery cells to be fed to the set up was empirically determined to be 8. During two occasions, exothermic reactions appeared to have taken place. This was most probably due to a high concentration of volatile components. For that reason, the ventilation rate was increased, resulting in a lower temperature of the sieving table of approximately 100 °C and no additional exothermic reactions for the remaining battery cell feeds. After all battery cells were added, the setup was operated for another 30 minutes to obtain most of the products.

During trials 3 and 4 no extensive emission sampling setup was used but the real time UFP monitor showed that there was UFP emission during the trials. Furthermore, the emission of volatile organic compounds was determined by capturing the atmosphere with a cannister on top of the activated carbon filters for later analysis.

Description of LFP trials

The last two trials involved large prismatic LFP battery cells that were about 1975 g in weight each. For both trials, a total of 5 LFP cells were processed. In trial 5, LFP batteries with a low SoC were shredded and in trial 6 LFP batteries with a high SoC were shredded. In both trials these cells are without casing. The battery cells that were used for these last two trials are shown in Figure 7.

Figure 7: The prismatic LFP battery cells that were used for trials 5 and 6.

For trials 5 and 6, it was decided that due to the large size of the battery cells that every 5 minutes a battery would be added to allow some time to process each battery. After the addition of the first LFP cell in trial 5, the temperature of the shredder was 25 °C, which gradually increased up to 31 °C after addition of the final battery. The temperature of the sieving table started at 79 °C. During the trial the temperature of the sieving table decreased to about 70 °C. The CO_2 concentration during the trial was rather stable around 10%. Also, the oxygen concentration became relatively stable around 5.5-6% after decreasing from 6.9% when the first battery was shredded. Approximately 11 minutes after adding the first battery to the setup, the first coarse particles and black mass was collected, indicating that the residence time is approximately 10 min. No exothermic discharges were observed during comminution of the LFP cells. The setup was operated for another 15 minutes after the addition of the final battery to collect most of the solid and liquid product.

At the start of trial 6 when the first battery was shredded, the temperature of the shredder was at 28 °C, which gradually went up to 33 °C after the last battery was shredded. The sieving table was relatively warm at 94 °C and the ventilation rate was increased to process the larger volume of the electrolyte solvents with the large battery cells. The remainder of the trial the sieving table had a temperature between 80-85 °C. The CO_2 concentration was quite stable between 11-12% with a low oxygen concentration just above 4% during the trial. Nine minutes after the addition of the last battery, some fumes coming out of the activated carbon filter were observed. No exothermic discharges were observed, and the setup was operated for another 20 min after the final battery was added to collect most of the solid and liquid product.

The UFP count was measured, and the volatile organic compound emission was sampled during trials 5 and 6 using a UFP monitor and cannister, respectively. The measurements showed that there was UFP emission during the trials. Similar to the NMC trials, elongated operation of the setup after finishing, resulted in the collection of additional solid product.

3.3   Analytical techniques used on product streams

After the trials, various product streams were obtained of which different samples were taken to TNO for analysis. For the assessment of the process, the main interests are to determine the black mass recovery efficiency and to determine the electrolyte removal efficiency. In addition, it is of interest to study the influence of SoC of the battery, battery chemistry, and the presence of casing, as these can affect the separation and recovery of materials and help to optimize the pretreatment process.

Various analytical techniques are employed to resolve the (chemical) composition, size distribution, and morphology of the various products. These analyses show how the changed parameters of the various trials can affect the product composition and product distribution. The analytical techniques that have been employed and the information these techniques can give will be listed here below.

Inductively coupled plasma mass spectrometry (ICP-MS) is an accurate technique that is able to quantify the elemental composition of a sample. This technique is commonly used to quantify metals, but also other elements can be quantified. Using this technique the material streams of the trials can be examined and metal content in the black mass (containing the valuable cathode active material metals), coarse particle stream and condensate is determined. This technique allows determination of the quality of the black mass (valuable metal content) and how much black mass will end up in the coarse particle stream and condensate.

Thermogravimetric analysis (TGA) is a technique that is complementary to ICP-MS. This technique relies on accurately weighing a sample while heating it over time. In this process, volatile compounds will evaporate and plastics/polymers and related molecules will decompose. When this technique is coupled with gas chromatography mass spectrometry (TGA-GCMS), the different compounds present in the sample can be identified and quantified. This method will be used to determine the organic components present in the black mass and show if the charge state or presence of the casing has an influence on the organic materials in the black mass. In addition, it can show how much the total content of metal(s) (salts) and graphite is in the black mass.

Scanning electron microscopy (SEM) is a technique that enables the determination of the size, shape, and texture of a material. When working with mixtures of compounds, it can also determine the size distribution and material/elemental distribution of a sample. This technique allows to make images of materials at the microscopic level. Images can be taken using secondary electrons (SE), which can show the morphology of a material or images can be taken with backscattered electrons, which gives information on the different elements in the sample and their distribution. This technique allows us to determine the particle size distribution within the black mass and how large the particles containing the valuable metals are. This knowledge can help in optimizing the sieving process of the pretreatment setup to obtain more or higher quality black mass.

Gas chromatography mass spectrometry (GC-MS) is a technique to identify and quantify organic molecules within a sample. With this technique the composition of the condensate containing electrolyte solvents and other compounds can be determined. Furthermore, this technique can show if and which volatile compounds/solvents still remain in the solid products obtained, and could help to study the efficiency of the electrolyte removal during the pretreatment process. In addition, it can be used to analyse the canisters that were used to sample the atmosphere. With this analysis the emission of volatile organic compounds can be determined that were in the atmosphere during trials 1 and 2.

4. Results and Discussion

4.1 Mass balance

In the objective to assess the pretreatment process setup, one of the key aspects that will be covered in the mechanical trials is the determination of the mass balance. A full mass balance of the process will assist in the determination of the black mass recovery efficiency, which is the most valuable material stream of the process. In addition, it provides insights into the complete material flow of the process. All output materials are collected and their mass and chemical composition are determined. This provides insights into the material flow and in which material stream the different components of a spent lithium ion battery (LIB) will end up in. The three main fractions collected in the process are the fine particle stream (black mass), the coarse particle stream, and the condensate fraction. In addition, for trials 1 and 2, particles emitted in the atmosphere are collected on various filters and the total emitted weight will be estimated based on mass collected on filters in combination with the ventilation rate.

NMC batteries

During the first trials, a total of 58 NMC battery packs were shredded divided over three batches with different SoC: 20 batteries with high SoC (8629.0 g), 21 with unknown SoC (9072.3 g), and 17 batteries with low SoC (7377.5 g). As full separation of the batches in the machine is not feasible, the mass balance is made up for the three batches of NMC batteries together. The total mass of the battery feed is 25 078.5 g, see Figure 8 and Table A1 (appendix).
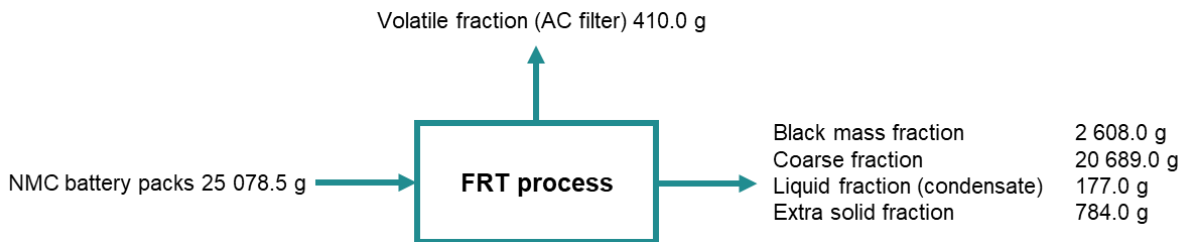

Figure 8: Schematic diagram of material streams and mass balance for the NMC-trials. Mass loss in NMC trials = 410.5 g.

Of the three main material output streams most of the mass is collected in the coarse particle stream with a total weight of 20 689.0 g. The second largest material stream is the black mass fraction of 2 608.0 g. The collected condensate is only a small part of the weight with 153.0 g. After the trial, extra solid fraction (784.0 g) and condensate (24.0 g) were collected from the setup by FRT. Furthermore, the activated carbon filters that were placed subsequent to the condensation unit of the setup had a significant weight gain of in total 410.0 g showing that the condensation process is capturing not all of the volatile components and that these end up in the activated carbon filters (AC filters). The combined material that was collected later and on the activated carbon filters adds up to 1 218.0 g (784 g + 24 g + 410 g), which is a significant portion of the total mass of the battery feed. The total mass collected in all the material streams adds up to 24 668.0 g, which is ~98.4% of the battery feed. This leaves a net balance of 410.5 g, which is not collected in the different material streams. In the process of collecting the condensate, an estimated amount of 30-40 g of material was spilled, which for a part explains the mass balance not adding up to a 100%.

NCA battery cells

During the third and fourth trials, 316 NCA batteries without casing (14 883.0 g) were shredded divided over two batches with different SoC: 156 batteries with a high SoC (7 347.0 g) and 160 batteries with a low SoC (7 536.0 g) with an average weight of 47.1 g per battery. The mass balance is shown in Figure 9 and Table A2 (appendix).

Volatile fraction (AC filter) 557.5 g

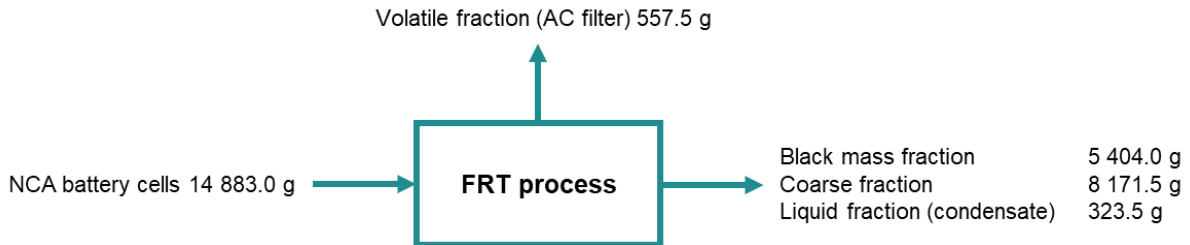| NCA battery cells 14 883.0 g | → | **FRT process** | → | Black mass fraction | 5 404.0 g |
| | | | | Coarse fraction | 8 171.5 g |
| | | | | Liquid fraction (condensate) | 323.5 g |

Figure 9: Schematic diagram of material streams and mass balance for the NCA-trials. Mass loss in NCA trials = 426.5 g.

Similar to the NMC trials, most of the mass in the NCA trials is collected in the coarse particle stream (8 171.5 g). However, the black mass (5 404.0 g) to coarse fraction ratio is significantly higher for the NCA trials, due to the lack of casing which typically ends up in the coarse fraction. Although the condenser was improved for trials 3 – 6, still a large weight gain was observed in the activated carbon filters (557.5 g), which was a larger mass increase than the collected condensate (323.5 g). The total output material collected adds up to 14 456.5 g, which is 97.1% of the battery feed. This leaves a net balance of 426.5 g, which is lost in the process.

LFP battery cells

During the fifth and sixth trials, 10 prismatic LFP batteries without casing (19 751.0 g) were shredded divided over two batches with various SoC: 5 batteries with a high SoC (9 828.5 g) and 5 batteries with a low SoC (9 922.5 g). The mass balance is shown in Figure 10 and Table A3 (appendix).

Volatile fraction (AC filter) 439.5 g

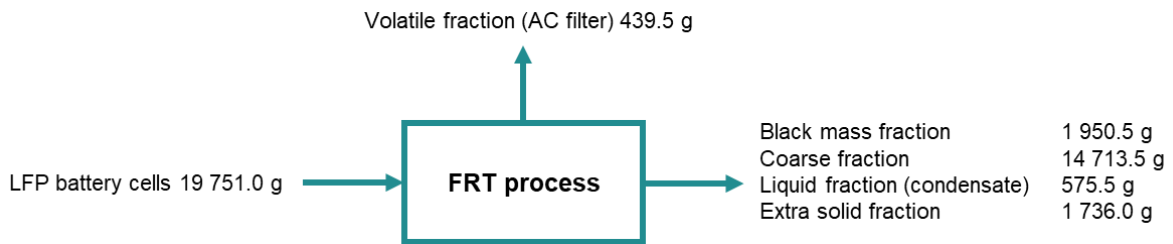| LFP battery cells 19 751.0 g | → | **FRT process** | → | Black mass fraction | 1 950.5 g |
				Coarse fraction	14 713.5 g
				Liquid fraction (condensate)	575.5 g
				Extra solid fraction	1 736.0 g

Figure 10: Schematic diagram of material streams and mass balance for the LFP-trials. Mass loss in LFP trials = 336.0 g.

For the LFP trials, a relatively high black mass to coarse fraction is expected, similar to the NCA trials, as no casing was present. However, by far most of the mass is collected in the coarse fraction (14 713.5 g) and much less black mass (1 950.5 g) was collected. For these trials, it was observed that a higher percentage of the volatile fraction ends up in the condensate (575.5 g) than in the activated carbon filters (439.5 g), when compared with the previous trials. After the trials, again, a significant amount of solid material (1 736.0 g) was collected by FRT, indicating that the solid fraction of the LFP batteries has a high residence time in the pretreatment setup before it is collected. The total amount of material collected adds up to 19 415.0 g, which is 98.3% of the battery feed. This means that 336.0 g of material is lost in the process.

To explain the negative net mass balances in the different trials, sources of material loss should be considered. One plausible explanation is that in the dead volume of the setup used for the battery pretreatment some of the mass remains. However, FRT was able to collect additional material after the trials were performed, which was added to the mass balance. In addition, material could have been lost due to the emission of particulate matter or vapours. A third source of weight loss could be the emission of non-condensable gases or vapours, like CO_2 or H_2O. To prevent any explosions or fire risks in the battery shredding setup, an inert atmosphere is used, which lowers the concentration of O_2 in the setup. In ambient atmosphere an O_2 concentration of ~21% is found, while throughout the trial a O_2 concentration of 5 +/- 2% is measured. This remaining oxygen could still react with hydrocarbon materials during the exothermic battery shredding process. That is exactly what is observed and an increase in the CO_2 atmosphere was measured with a concentration of 10 +/- 1% (ambient concentration ~0.04%). This indicates that part of the hydrocarbon content of the battery is burned in the shredding process with release of CO_2 and H_2O, or that the electrolyte solvents decompose in the shredding process with release of CO_2 and dialkyl ether products. These two compounds can leave the setup as gases resulting in mass loss (assuming the H_2O does not condensate or adsorb on the activated carbon filter).

4.2   Particulate matter and VOC emission included in mass balance

Emission of VOCs

To assess how much and what type of material is lost due to emissions during the process, volatile organic compounds (VOCs) and particulate matter (PM) are sampled during the NMC battery trials. Sampling setups were placed, at three different locations, setup 1, 2 and 3 (see Figure 11). Each sampling setup consisted of a cannister which collects the atmosphere over a controlled period of time and filters that capture (PM).
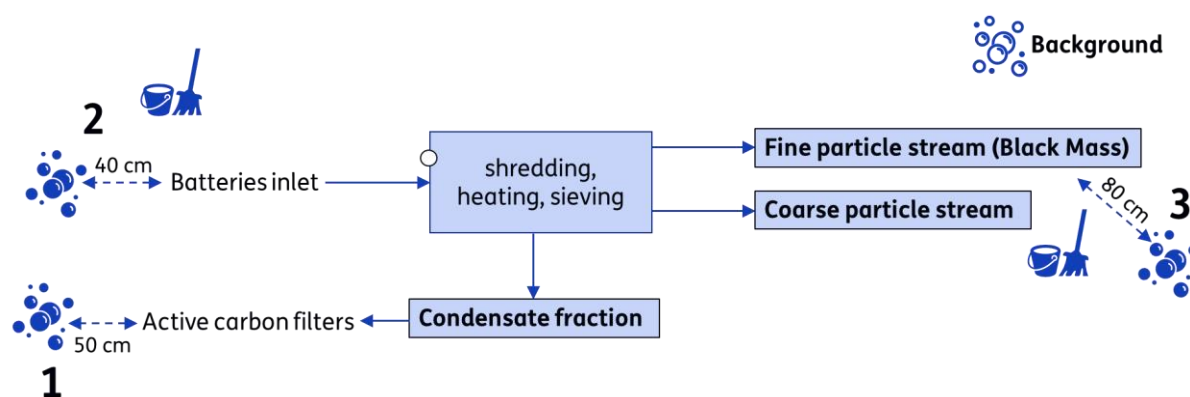

Figure 11: Schematic representation of the battery pretreatment setup and material fractions collected with the location of the three sampling setups 1, 2, and 3 indicated.

Afterwards, the gas collected in the canisters was analysed by GC-MS, which results in an average emission over the sampling time of various VOCs. Initial semi-quantitative GC-MS analysis showed that organic compounds were present, with a composition similar to what was found for the condensate of the NMC trials: it contained mostly dimethyl carbonate (DMC), followed by a low amount of ethyl methyl carbonate (EMC) and traces of diethyl carbonate (DEC) (see also section 4.30). Because the DMC was the most abundant of the VOCs that was being emitted, its emission at the different setups was quantified and was then compared with the background level. The background level of DMC that was measured overnight was 0.2 mg/m³. The DMC concentration at setups 1 and 3 was similar with 2.9 and

3.4 mg/m^3, respectively. The DMC concentration at the battery inlet of the pretreatment setup (setup 2) had the highest concentration at 8.0 mg/m^3. Additionally, during the NMC battery trials, emission of fumes coming out of the outlet of the activated carbon filter was observed. Therefore, an additional cannister was sampled close to sampling setup 1 during fume emissions to determine what was emitted. This additional cannister showed a concentration of DMC of 10.9 mg/m^3, which is only slightly higher than for the other cannisters. This indicates that the fumes being emitted did not contain significant more VOCs and that the emission of water is more likely, which is not adsorbed on the activated carbon filters and not detected by GC-MS.

An estimation of the total mass of VOC in the form of DMC that was emitted can be calculated when the total volume of the room and ventilation rate are known. Because the volume of the hall is known, it is possible to calculate the ventilation rate of the hall based on the time it takes for the measured UFP concentration to return to the background concentration. The ventilation rate was calculated to be approximately 1.5 air changes per hour (ACH), indicating that the atmosphere of the room is exchanged 1.5 times every hour. The total time of the NMC trial was approximately 2 h and the room volume is 300 m^3, giving a total volume of 900 m^3. The highest average DMC concentration that was measured was 8.0 mg/m^3 which results in a maximum emission of DMC around 7.2 g, based on the assumption that the air is perfectly mixed. These results indicate that the VOC emission is only a small part of the loss in mass of the NMC trial.

Emission of particulate matter

Next to the emission of VOCs, also the emission of particulate matter (PM) was measured using different types of filters at the three measurement setups. The material that was collected on these filters was subjected to various analytical techniques to determine the amount of PM that was collected and what the composition of this material is. The choice of these different type of filters relates to the type of analysis that was performed. Gold filters are used as substrate for SEM analysis and Teflon filters are used for ICP-MS analysis of the PM. The detection of PM in the background was determined prior to the NMC trial. This showed a PM background concentration of 0.0079 mg/m^3. The concentration of PM emission was determined at measuring setup 1, 2, and 3, similarly as for the VOC emission. The results showed that the highest PM concentration was found at setup 1 (after activated carbon filters) at 1.91 mg/m^3 and slightly lower concentration at setups 2 and 3 with 0.63 and 0.65 mg/m^3, respectively. In a similar calculation as shown for the VOC emission above, an approximate maximum PM emission can be determined based on the PM concentration of setup 1, resulting in a PM emission of 1.72 g over the timeframe of 2 h of the NMC trial. These results thus also indicate that the PM emission is a small part of the loss of mass in the NMC trial. It is observed that the PM emission after the activated carbon filters is about three times higher than for the other two measurement setups, while it is expected that activated carbon filters can filter both VOC and some PM. However, it has been described that activated carbon filters can release small particles of carbonaceous material from the filters itself (Li et al., 2023), which could explain the higher emission of PM in setup 1.

ICP-MS and SEM analysis of air sample filters

To gain more insight into the composition of the PM that is collected during the NMC trial, the PM was analysed with ICP-MS and SEM analysis. The metal content of the collected PM on the Teflon filters was determined using ICP-MS. The material from the filter of the background did not show any metal content, because the total mass on the filter was too low to obtain metal concentrations above the detection limit. The PM collected on setups 1, 2, and 3 all showed the presence of various metals. The approximate metal loading per gram of PM is shown in Table 2. This table shows that the metals of the cathode active material of NMC batteries are detected and that these metals make up to a few % of the

mass of the PM, indicating that some of the material of the black mass is being emitted during the operation of the pretreatment setup.

Table 2: The CAM loading per gram of PM collected at the different setups.

	Li (mg/g PM)	Ni (mg/g PM)	Mn (mg/g PM)	Co (mg/g PM)
Setup 1	1.4	3.8	1.8	1.4
Setup 2	2.5	6.7	3.2	2.7
Setup 3	3.2	8.3	4.1	3.3

Next, the morphology and elemental composition of the surface of the PM collected on various gold filters was analyzed by SEM. It was shown that the PM collected in the background contained particles that were mainly in the size range of 1-10 µm and that have a composition that was rich in the following elements: C, O, Al, Si, Ca, Na and also containing some K, Mg, Cl, Ti, Fe, Cu. These elements are not the main constituents of battery materials. These elements are more common in soil and minerals. The PM collected on the different setups contained somewhat larger particles around 5-40 µm and also displayed different elemental composition (see SEM images in the Appendix). There were many particles that consisted mainly of C, O, F and P, (indicating presence of graphite and electrolyte salts) but also particles that consist of Al, K, Ca, Mn, Co and Ni and Fe (indicating the presence of particles of dust, steel, and cathode active materials). These results indicate together with the ICP-MS results that some black mass material (graphite and cathode active materials) are being emitted. Analysis of approximately 1000 particles on the filter of setup 1 using an automatic search analysis showed that in the size range of 5-30 µm about 10-20% of the particles contained CAM elements (Ni, Mn, Co). Most of the other particles consisted of a carbon containing material indicative of mostly graphite and the presence of binder material (due to the presence of fluorine) or other organic materials.

4.3   Electrolyte removal during the pretreatment process

In the shredding process, short-circuiting of the batteries in combination with mechanical force/friction results in heating of the battery materials. In the closed sieving table, the battery materials are heated by external heating as well. This heat is used to evaporate the electrolyte solvent, which is captured in the condenser to separate the liquid fraction (electrolyte solvents) from the solid fraction. By analysing the mass balance in combination with the composition of the liquid fraction (condensate) and solid fractions, it is possible to estimate the efficiency of the electrolyte removal from the solid fractions. Because it was not possible to determine the electrolyte quantity or composition of each of the studied (end-of-life) batteries prior to the shredding process, it is challenging to fully quantify the electrolyte solvent removal efficiency.

In order to determine the efficiency of the electrolyte removal, it is useful to compare the amount of collected condensate (liquid fraction) with the wt% of electrolyte that is expected for these battery types if that data is available. In addition, the composition of the electrolyte solvents are determined, since different electrolyte solvents have different boiling points. Solvents with a higher boiling point will be more difficult to quickly evaporate than solvents with a lower boiling point. Furthermore, the solid material fraction is analysed to determine what the volatile organic component (electrolyte solvent) content is within these materials. During burning of organic materials of the battery, such as plastic or electrolyte solvents, water is released which could also end up in the condensate. Because GC-MS cannot detect

water, a Karl Fischer titration method was employed to determine the water content within the condensates of the various trials.

NMC batteries

In literature, it is described that NMC batteries contain around 8 wt% of volatile components of which most comprises electrolyte solvents (Diekmann et al., 2017). Interestingly, the collected condensate is only about 1 wt% of the total output material, indicating that some electrolyte solvent is lost. Even when considering that all mass collected in the activated carbon filters is due to electrolyte solvents, it adds up to only 3 wt%. To further assess the electrolyte removal, the composition of the electrolyte solvents was measured, because different solvents have various boiling points and are thus more or less facile to evaporate, see Table 3 for the results.

Table 3: The electrolyte solvent composition measured in the various output streams of the NMC trial using GC-MS.

		DMC (b.p. 90 °C)	EMC (b.p. 101 °C)	DEC (b.p. 126 °C)	EC (b.p. 243 °C)
NMC trial	Condensate	>90%	~5%	~1%	0%
	Coarse	~90%	~10%	~1%	0%
	Black mass	TGA: 1.5-2.5 wt% consists of electrolyte			

The organic compounds within the condensate were analysed using GC-MS analysis. Common electrolyte solvents used for lithium ion batteries are dimethyl carbonate (DMC), ethyl methyl carbonate (EMC), diethyl carbonate (DEC), or ethylene carbonate (EC). The analysis was performed semi-quantitatively and showed that over 90% of the condensate consists of DMC. Small amounts of EMC were also detected as well as traces of DEC. Of the detected solvents in the condensate DMC has the lowest boiling point (90 °C) followed by EMC (101 °C) and DEC (126 °C). EC has a considerably higher boiling point (243-244 °C). The temperature of the sieving table was around 75 +/- 5 °C during the trials. Therefore, the low content level of DEC, EMC, or EC in the condensate fraction can be explained by their boiling point, which is higher than the temperature of the sieving table. In case these solvents cannot evaporate during the residence time in the sieving table, these would end up in the solid coarse or black mass fractions. Using the Karl Fischer titration method the water content in the condensate was determined to be ~1 wt%, indicating that burning of organic material during the shredding process takes place.

However, the solid materials obtained in the trial appeared dry for the eye, suggesting that the solids did not contain noticeable amounts of electrolyte solvents. To quantify the volatile content in the black mass, it was analysed using TGA. Unfortunately, TGA analysis could not be performed for the coarse fraction to get a more complete picture due to its heterogeneity preventing good sampling. Therefore, a sample of the coarse fraction was collected and heated in a sealed pot from which a sample could be taken from the headspace for GC-MS analysis. The combination of these two analyses provides a semi-quantitative result on how much and which electrolyte solvents end up in the solid fractions. The GC-MS analysis of the headspace of the coarse fraction showed that three different solvents are present. The most abundant solvent is DMC (~90%), followed by EMC (~10% of total solvent content) and a small amount of DEC. It appeared that, unexpectedly, the coarse fraction obtained from the NMC batteries with a high SoC, have a somewhat higher loading of electrolyte solvent than from the batteries

with a low SoC. This was unexpected, because the batteries with a high SoC would release more heat during the shredding step, which assists electrolyte solvent evaporation.

The black mass fractions obtained from the two different SoC were both measured three times with TGA to obtain a more reliable result. Within the volatile region of heating during the TGA analysis (heated up to 250 °C) for all measurements, a weight loss was observed between of 1.5 - 2.5%. This indicates that around 2 wt% of the black mass consists of electrolyte. It is conceivable that during the shredding, shaking and sieving process the electrolyte is spread over the battery materials and that a similar percentage of electrolyte ends up on the coarse fraction. Although the TGA data shows a slightly lower weight loss up until 250 °C for the batteries with a high SoC compared to the batteries with a low SoC (~0.5 wt% more), it is difficult to solely address this phenomenon to a higher residual energy of the batteries with a high SoC. The lower amount of solvents present in these materials can also be (partially) explained by a higher temperature of the sieving table during the trial with batteries with a high SoC compared to the trial with batteries with a low SoC (~10 °C).

Another explanation of the lower than expected electrolyte solvent retrieval during the shredding process is due to thermal decomposition of the electrolyte solvents (Fernandes et al., 2019). In this process, gases like CO_2 are formed, which are not captured and released from the setup. Furthermore, the Karl Fischer titration method showed that water is formed in the process. This can leave the setup if it is not effectively condensed, because activated carbon filters are not optimized to adsorb water.

NCA battery cells

NCA batteries without casing were used for these trials. For trials 3 – 6, FRT had updated their condenser, in order to more efficiently condense the vapor, which would lead to a lower loss of the condensate in the activated carbon filters. Based on the mass balance, the condensate of the liquid fraction contains ~2 wt% of the total battery input. The part of the liquid fraction that is captured in the activated carbon filters is 3.7 wt% of the battery feed. With the assumption that a large part of the weight gain in the activated carbon filters is from electrolyte, then this data suggests that the electrolyte in these trials is well separated from the solid fractions. The electrolyte content and composition in the output streams of the NCA trial was studied and the results are shown in Table 4.

Table 4: The electrolyte solvent composition observed in the various output streams of the NCA trial.

		DMC (b.p. 90 °C)	EMC (b.p. 101 °C)	DEC (b.p. 126 °C)	EC (b.p. 243 °C)
NCA low SoC	Condensate	~75%	~25%	~1%	0%
	Coarse	~75%	~25%	~1%	0%
	Black mass	TGA: 1.0-1.5 wt% consists of electrolyte			
NCA high SoC	Condensate	~40%	~50%	~10%	0%
	Coarse	~60%	~30%	~10%	0%
	Black mass	TGA: 1.0-1.5 wt% consists of electrolyte			

The organic compounds in the condensate of the NCA trial were analysed using GC-MS to determine the composition, which will assist in determining what temperature is needed to evaporate the solvents. It was found that, similar to the NMC trials, the three main solvents that condensed are DMC, EMC, and

DEC. Using a semi-quantitative GC-MS analysis, it was found that the condensate from the trial with batteries with a low SoC have DMC as main component (~75%) and EMC (~25%) and DEC (~1%) as minor components. Interestingly, the ratio of these three solvents was different for the trial with batteries with a high SoC: DMC (~40%), EMC (~50%) and DEC (~10%). This difference in ratio between solvents was not expected, since for both trials identical battery cells were used that only differed in SoC. The batteries with high SoC were shredded prior to the batteries with low SoC for the NCA batteries. This result might indicate that the condensation process takes relatively long and that first the solvents with higher boiling points condensate (DEC and EMC) and later DMC and that this process takes longer than the trials themselves. In the next trial then with NCA batteries with a low SoC finally the DMC condenses from the previous trial, which could explain why for this trial a higher ratio of DMC compared to the other solvents is observed in comparison with the trial with high SoC batteries. The water content of the condensate was determined to be approximately 0.5 wt% using the Karl Fischer titration method, indicating that also here burning of organic material during the shredding process took place.

The presence of electrolyte solvents within the solid fractions was determined again by TGA analysis of the black mass in threefold and headspace GC-MS analysis of the coarse fraction. The TGA data of the black mass from the NCA batteries showed that 1-1.5% of the mass is lost in the volatile region (up to 250 °C) for both the batteries with a high and low SoC. 1 wt% of the black mass corresponds to 54 g for the NCA batteries. This is a lower percentage than for the NMC batteries (2 wt% corresponds to ~50 g), which indicated that (most of) the electrolyte was removed from the solid fraction.

The identification of the compounds in the volatile fraction in the coarse fraction was performed using headspace GC-MS. This semi-quantitative analysis showed that in the coarse fraction only a small quantity of three different solvents was detected. The main component is DMC, with less EMC and even less DEC. This was the same for both different coarse fractions collected showing that the SoC does not influence the remaining solvent ratio within the coarse fraction. The sieving table temperature was also not identical for both NCA trials, which might suggest that the sieving table temperature for both trials does not affect the solvent composition in the condensates.

LFP battery cells

Large prismatic LFP batteries of around 2 kg were used for the last two trials. It depends on the cell type and manufacturer how much electrolyte is present in these LFP cells, but it is often argued by industrial parties to be more than in NMC or NCA cells. The two different trials with batteries of different SoC used, showed a difference in condensate recovery. For the low SoC batteries, around 2 wt% of the battery feed material was condensed as electrolyte solvents. Another 1.6 wt% of mass was collected in the activated carbon filters. For the high SoC batteries, a higher electrolyte recovery in the condensate was obtained with ~4 wt% of the battery feed material. Also, a higher loading was observed on the activated carbon filters with ~3 wt% of the input mass. This result, that for both batteries with a low and high SoC a low electrolyte recovery is observed, can indicate that electrolyte ends up in the solid fractions. The electrolyte solvent content and composition was studied of the various output streams of the LFP trial, see Table 5.

To gain a better understanding of why a relatively low electrolyte recovery was obtained, the composition of the condensate was determined using GC-MS. Such analysis can reveal if for example more solvent with a higher boiling point is present compared to the previous trials. This semi-quantitative analysis showed that the composition of the recovered condensate from the batch of the batteries with a low SoC is slightly different than from the batteries with a high SoC.

Table 5: The electrolyte solvent composition observed in the various output streams of the LFP trial.

		DMC (b.p. 90 °C)	EMC (b.p. 101 °C)	DEC (b.p. 126 °C)	EC (b.p. 243 °C)
LFP low SoC	Condensate	~50%	40-45%	~10%	0%
	Coarse	~25%	~50%	~25%	0%
	Black mass	TGA: 5.5 wt% consists of electrolyte of which 1 wt% is EC			
LFP high SoC	Condensate	~40%	~50%	~10%	0%
	Coarse	~45%	~50%	~5%	0%
	Black mass	TGA: 4.3 wt% consists of electrolyte of which 1 wt% is EC			

The batteries with a low SoC resulted in a condensate that has DMC as main component (~50%), and EMC (40-45%) and DEC as minor components (~10%). The condensate obtained from the trial with batteries with a high SoC has EMC as main component (~50%) and DMC (40%) and DEC (10%) as minor components. Since there was no clear exothermic discharge observed from any of the shredded LFP batteries during the trials, it is not expected that the SoC of the batteries has had a large influence that can explain the observed difference. The difference in solvent ratio in the condensate can be better explained by the temperature of the sieving table during the trials. In the trial with batteries with a low SoC the sieving table was about 10 °C lower than for the trial with a high SoC, which prevents quick evaporation of the solvents with a higher boiling point (EMC/DEC). The condensates of the LFP battery trials were also analysed with the Karl Fischer titration method. It was found that these had water contents of around 0.3 wt%, indicating that some burning of organic material took place.

The solid fractions were analysed semi-quantitively by GC-MS to determine the remaining solvent and solvent ratio on them. It was noticed during the analysis that the solid fractions of the LFP trials had a clear smell, whereas the solid materials from the NMC and NCA trials did not. This indicated that a larger amount of solvents were still present in the solid fractions compared to the NMC and NCA trials. Headspace GC-MS analysis of the coarse fraction of both LFP trials showed indeed that a high loading of solvents was present on the particles in the coarse fraction, which was approximately five times higher compared to the NMC and NCA trials. For the LFP batteries with low SoC, the main solvent present was EMC (~50%) with similar amounts of DMC (25%) and DEC (25%). The batteries with high SoC also showed EMC as main component (~50%) and more DMC (~45%) than DEC (~5%).

TGA analysis of the black mass of both LFP trials in threefold gave a more quantitative result. The low SoC black mass obtained showed an average 5.5 wt% loss in the volatile region (up to 250 °C), whereas the high SoC black mass had an average 4.3 wt% loss. These values are significantly higher than for the NMC and NCA batteries. Because these values are higher than for the NMC and NCA trials, the volatile components could be identified by coupling the TGA analysis with GC-MS analysis. It was shown that DMC, EMC, and DEC were present, but also ethylene carbonate (EC, boiling point 243-244 °C). The EC was quantified for both LFP black mass fractions and both contain 1 wt% of EC. This high boiling solvent is not removed during the sieving process due to a too low temperature of the sieving table.

It is difficult to compare the results of the NMC and NCA trials with the LFP trials, because the LFP batteries have three variables that are different and can influence the electrolyte removal. The LFP batteries are considerably larger cells, contain relatively more electrolyte and the solvent mixture have a higher boiling point than for the NMC and NCA batteries. Although more electrolyte remains in the

solid fractions of the LFP trials compared to those of the NMC and NCA trials, it is not possible yet with the current data to determine which of these variables has the largest influence on the efficiency of the electrolyte removal during the pretreatment process.

Overall findings

The process discussed in this report can treat charged batteries and battery cells. For that reason, per type of battery or battery cell, a batch of charged batteries and a batch of uncharged, or at least significantly lower voltage, batteries were shredded to make a comparison.

In the case of NMC batteries, an exothermic discharge was observed during comminution of the batteries with a high SoC, which was not in the case during the trial with low SoC battery packs. These observations show that shredding of batteries with a higher SoC is indeed more exothermic, meaning that they release more heat during shredding. The average CO_2 and O_2 concentration was similar for both trials. However, the temperature of the sieving table is important for the electrolyte removal as well and was rather difficult to control to make a good comparison: the trial involving batteries with a low SoC had a temperature of the sieving table that was nearly 10 °C lower than for the trial with a high SoC.

In the NCA trials with batteries with a high SoC significantly more exothermic discharges were observed compared to the trial with low SoC batteries. Furthermore, a higher average temperature of the sieving table and a higher concentration of CO_2 was observed for the trial with the high SoC batteries compared to the low SoC batteries, also indicating a more exothermic reaction for batteries with a high SoC. Although there were no exothermic discharges in trial 5 or 6 during the shredding of the batteries, it was observed that there were some differences.

In the trial with the high SoC LFP batteries, a higher temperature of the sieving table and a higher CO_2 concentration were observed compared to the batteries with a low SoC. This can indicate that more energy and heat is released with the batteries with a high SoC. Combining all observations and results above, it is difficult to conclude what exact impact the residual energy of batteries and battery cells have on the process other than the occurrence of exothermic discharges and increased temperature. As the temperature of the sieving table was not stable during the trials, it was not possible to quantify the impact of the residual energy to the electrolyte removal. However, these results do indicate that the current pretreatment process is not sufficiently optimized for the efficient removal of the electrolyte solvents from batteries and battery cells.

4.4   CAM recovery efficiency

Another important research question is how much of the cathode active materials in the batteries are recovered in the black mass fraction using in the pretreatment process. In other words, how much cathode active material is lost or trapped in the coarse fraction during the separation process? To address this question, multiple analytical techniques have been used to characterize both the fine black mass and coarse fraction to determine their composition as well as size and morphology distribution.

NMC trials

The trials involving NMC batteries consisted of batteries with casing. During the shredding and separation process, the CAMs and graphite on the anode are concentrated in the black mass fraction, while the plastics and metal pieces generally end up in the coarse fraction. This explains why for these trials, by far most of the mass ends up in the coarse fraction. The fine graphite and cathode powders in NMC batteries make up about 25 wt% of the cell of a battery (Diekmann et al., 2017). For these trials,

the black mass fraction is almost 8 times lower in mass then the coarse fraction, which could be expected due to the presence of casing in the coarse fraction. To determine what materials ends up in the black mass fraction, ICP-MS analysis was used to quantify the metals and phosphorus in this fraction.

A number of different elements which were expected in the black mass fraction were quantified. The black mass produced from batteries with a low SoC had a sum of cathode active materials (Li, Ni, Mn, Co) of 26 wt%. The main other elements detected were aluminium (2.6%) and copper (4.5%) and lower amounts of iron and phosphorus (both below 1%), which together all adds up to 35 wt% of metal and phosphorus content in the black mass. The remaining mass consists mainly of carbon containing materials (graphite, binders like PVDF, conductive carbon, plastic particles, some electrolyte solvents), oxygen (present in cathode active material as oxides) and fluorine (present in PVDF binder and electrolyte salt), based on TGA, GC-MS and SEM analysis. TGA results down below will go into more detail about the carbon containing fraction. The black mass from the batteries with a high SoC contains a comparable sum of cathode active material (Li, Ni, Mn, Co combined is 22 wt%) compared to the black mass from the batteries with a low SoC. The total sum of metals and phosphorus is 30 wt%.

The black mass content that is still trapped in the coarse fraction was determined by ICP-MS analysis. However, the coarse fraction is a highly heterogeneous mixture of materials with different composition and size distributions. A representative homogeneous sample of this heterogeneous mixture was prepared through an ashing (incineration) procedure followed by a sieving step. In this ashing procedure, a relatively large sample (30-50 g) was heated in air to 800 °C, which resulted in a fine ash that contained larger steel particles (from battery casing). All carbon containing material (e.g. plastics, graphite) is burned off in this process and most of the metallic content is oxidized. After sieving of this ash (1.6 mm sieve), a fine ash fraction and steel fraction were obtained. This fine ash contains the cathode active materials, other metals (oxides) and other salts and can be easily used as homogeneous sample for ICP-MS analysis. The measured elemental distribution in the ash is then converted to metal content in the coarse fraction by taking the weight loss during the ashing procedure into account. The ashing procedure followed by ICP-MS analysis thus reveals the amount of cathode active materials that was trapped in the coarse fraction.

The coarse fraction from the batteries with low SoC contains a sum of cathode active materials (Li, Ni, Mn, Co) of 7 wt%, which is lower wt% than in the black mass fraction (26 wt%, see above). However, because the coarse fraction is much larger in mass compared to the black mass fraction, this means that a significant portion of the cathode active materials are still trapped in the coarse fraction. A similar finding was made when the coarse fraction of the batteries with high SoC was analysed and a sum of cathode active materials (Li, Ni, Mn, Co) of 5 wt% was found. The distribution of CAMs over the fine black mass fraction and the coarse fraction from 1 kg of batteries (summed and averaged of both low and high SoC batteries) is presented in Figure 12 and Table 6 (shown below discussing overall findings of the six trials). The distribution of CAMs in both solid fractions is derived from the elemental composition of these two fractions. It shows that per kg of batteries, 25 g of CAMs is retrieved in the black mass fraction and still 49 g of CAMs is trapped in the coarse fraction. This result shows that a large part of the valuable CAMs does not end up in the fine black mass fraction. In order to recover a larger part of the valuable CAMs in the fine black mass fraction from NMC batteries in casing, a change of the pretreatment process is thus required.
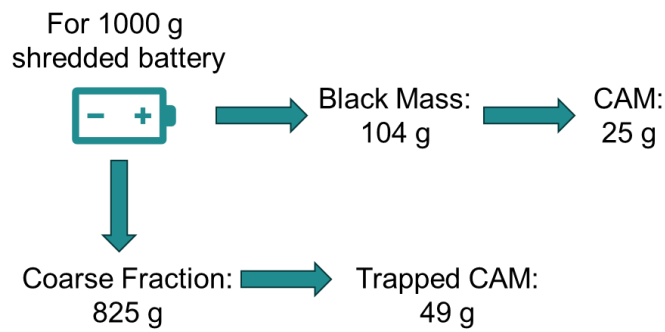
Figure 12: Mass distribution over the fine (black mass) and coarse fraction from 1000 g of NMC batteries with casing and the amount of CAMs in the black mass and trapped in the coarse fraction. This is calculated as an average of the batteries with a high and low SoC.

NCA trials

Analogous to the NMC trial output materials, the elemental composition of the black mass fraction and the coarse fraction from the NCA battery trials was determined. Since the NCA battery cells were not in casing, a higher black mass to coarse fraction ratio was observed in the mass of the output materials. The sum of the CAMs (Li, Ni, Co) in the black mass fraction of the batteries with low SoC adds up to 28 wt%, which is slightly higher than for the batteries with high SoC with 22 wt%. This is most likely due to a spillover from a previous non-related trial to this project performed with LFP batteries by FRT prior to the NCA trials as a significantly higher iron and phosphorus content is observed in the black mass fraction from the batteries with a high SoC (performed before trial with low SoC batteries) than for batteries with a low SoC. The total metal + phosphorus content for both these black mass fractions adds up to 31 wt%, indicating that the largest part of the mass is due to the presence of other materials, like graphite, plastic, binder, etc.

The elemental distribution of the (metallic) elements in the coarse fraction was also determined by ICP-MS after an ashing procedure, similar to that performed for the NMC trials. Compared to the NMC battery trials, the NCA trials' coarse fraction contains a significantly higher CAM percentage, which is explained by the lack of battery casing for these trials. The coarse fraction from the batteries with low SoC contains 20 wt% of CAM (Li, Ni, Co) and the coarse fraction from the batteries with a high SoC contains 17 wt% of CAM. The distribution of CAMs over the fine black mass fraction and the coarse fraction from 1 kg of batteries (summed from both low and high SoC batteries) is presented in Figure 13 and Table 6. The results show that per kg of batteries a similar amount of CAM ends up in the fine black mass fraction (92 g) as is trapped in the coarse fraction (104 g). Although the ratio of CAM that ends up in the black mass fraction compared to that in the coarse fraction is higher than that observed for the NMC trials, it is evident that a large part of the valuable CAM does not end up in the black mass fraction. Therefore, there is room for improvement of the pretreatment process to allow a larger part of the CAM to end up in the fine black mass fraction. The higher ratio of CAM presence in black mass compared to the coarse fraction for the NCA cells compared to the NMC battery packs could (partly) be explained by the presence of the casing in the NMC trials. However, from the trials preformed here, it is not possible yet to provide a conclusive explanation for this. Therefore, to study the influence of the casing on the separation of the CAM from the coarse fraction, more trials are required. For example, trials of the same battery chemistry/type with and without the presence of battery casing and more well-defined charging state.

For 1000 g
shredded battery

Black Mass: CAM:
363 g   92 g

Coarse Fraction: Trapped CAM:
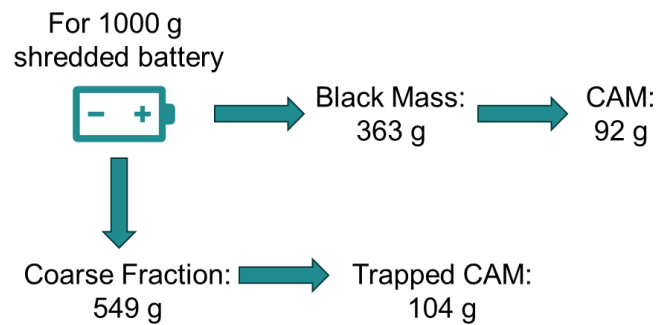549 g   104 g

Figure 13: Mass distribution over the fine (black mass) and coarse fraction from 1000 g of NCA batteries without casing and the amount of CAMs in the black mass and trapped in the coarse fraction. This is calculated as an average of the batteries with a high and low SoC.

LFP trials

The elemental distribution of the black mass fraction of the batteries with a low and high SoC was determined using ICP-MS, analogous to the NMC and NCA trials. The sum of CAM (for LFP batteries Li, Fe and P) in the black mass from the batteries with low SoC (22 wt%) and high SoC (28 wt%) are not identical, but this is for a large part explained by the spillover from the NCA trials, since a combined 6 wt% of Ni and Co is found in the black mass of the LFP batteries with a low SoC. LFP batteries do not contain Ni or Co, indicating that these elements originate from the NCA trials that were performed prior to the LFP battery trials. Similar to the NMC and NCA trials, most of the mass of the black mass consists of materials other than CAMs (e.g. plastics, binder, graphite), as a sum of ~35 wt% is found for metals and phosphorus.

By far most of the mass ended up in the coarse fraction. This is likely explained by the presence of remaining electrolyte solvents in the solid fractions (see section0 on electrolyte removal efficiency above), which makes the fine CAM fraction stick to the larger coarse particles during sieving. The ashed coarse fractions were also analysed by ICP-MS and the elemental composition of the coarse fraction was derived from those results. Similar to the NCA batteries, a high CAM content was found in the coarse fraction of the batteries with low SoC (21 wt%) and high SoC (18 wt%). The distribution of CAMs over the fine black mass fraction and the coarse fraction from 1 kg of batteries (summed and averaged from both low and high SoC batteries) is presented in Figure 14 and Table 6. The distribution of CAMs in both solid fractions here is derived from the elemental composition of these two fractions. The figure shows that per kg of battery material a sum of 170 g CAM is present of which 25 g ends up in the black mass fraction and by far most of the mass (145 g) is trapped in the coarse fraction. This result indicates that the current pretreatment process is not optimized for separating the CAM from the coarse fraction using this type of LFP battery cells. In particular, the presence of a larger amount of electrolyte solvents should be taken into account.

For 1000 g
shredded battery

Black Mass:
99 g

CAM:
25 g

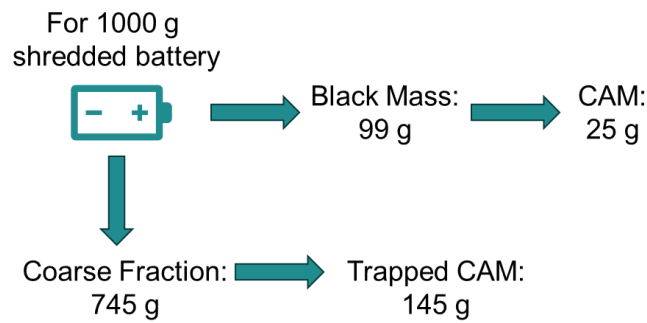Coarse Fraction:
745 g

Trapped CAM:
145 g

Figure 14: Mass distribution over the fine (black mass) and coarse fraction from 1000 g of LFP batteries without casing and the amount of CAMs in the black mass and trapped in the coarse fraction. This is calculated as an average of the batteries with a high and low SoC.

Overall findings

One of the sub questions for assessing the pretreatment process, is to study the influence of the casing and the SoC on the separation of the black mass (CAMs) and coarse fraction and material output. On the basis of the measured elemental distribution in the solid output materials of the various trials, see Table 6 describing the CAM content in various solid output streams, it is not possible yet to draw any hard conclusions on a clear effect of the SoC on the output materials. In principle, a higher SoC would give a larger energy release during the shredding process, which could result in a more efficient separation of the electrolyte and the solid materials. However, significant differences in elemental distribution were not observed between batteries with a high and low SoC. The obvious differences that were found for the elemental distributions between trials with batteries with a low and high SoC are explained well by the observed spillover of material between different trials into the next trial. This indicates that the residence time of some of the material is considerably longer than the time that is now used to obtain the output material after the last battery is added to the setup (15-30 min). Therefore, a longer operation time should be used between trials to ensure that (most of) the output material is removed from the setup to prevent any spillover. In addition, it was observed that the presence of electrolyte solvents has a negative impact on the CAM recovery in the black mass fraction. Furthermore, it is difficult to draw conclusions on the effect of casing on the separation of the CAM from the coarse fraction and its effect on the separation of the electrolyte solvents from the solid output material. In order to answer this question, more trials of identical battery type with and without the inclusion of casing should be performed.

Table 6: Distribution of cathode active materials in weight percentage and mass of cathode active materials per kg of batteries in the black mass and coarse fraction.

Trial parameters	Fraction	CAM (wt%)	CAM (g/1000 g batteries)	Division of CAM over material streams
NMC low SoC In casing	Black mass	26*	27	31%
	Coarse	7*	59	69%
NMC high SoC In casing	Black mass	22*	23	37%
	Coarse	5*	39	63%
NCA high SoC Dismantled	Black mass	22**	71	43%
	Coarse	17**	96	57%
NCA low SoC Dismantled	Black mass	28**	112	50%
	Coarse	20**	110	50%
LFP low SoC Dismantled	Black mass	22***	22	12%
	Coarse	21***	155	88%
LFP high SoC Dismantled	Black mass	28***	28	17%
	Coarse	18***	135	83%

* The selected cathode active materials here are Li, Ni, Mn, and Co summed. ** The selected cathode active materials here are Li, Ni and Co. Al is excluded, because only a small part of NCA is Al and it can also originate from Al foil of current collector. *** The selected cathode active materials here are Li, Fe and P.

4.5 TGA and GC-MS analysis of the black mass

The elemental distribution of the black mass fractions of the various trials and the presence of electrolyte solvents in the black mass fractions has been described in the previous sections. It was found that by far most of the mass that was collected in the black mass fractions, does not consist of metals, but mainly consists of carbon containing materials, like graphite, plastics, separator, and other (volatile) organic components. A technique complimentary to ICP-MS, which is able to qualitatively and quantitatively study the carbon containing material in a sample, is TGA coupled with GC-MS (see also description in section 3.3). To gain a better understanding of the composition and amount of materials other than CAMs in the black mass fractions, the fractions were analysed with TGA coupled with GC-MS. In a TGA analysis, a sample is heated to 1000 °C, and in different temperature regimes different type of components evaporate/break down/burn from which the quantity and identity of various components can be determined. The trajectory up until 800 °C is performed under inert atmosphere and from 800 – 1000 °C in air, which oxidizes the remaining sample. The regime until ~250 °C is called semi-volatile organic components (SVOC, e.g. solvents, water), from ~250-~800 °C is called the pyrolysis regime (plastics, other polymers) and above 800 °C all carbon containing material is burned off, which illustrates the presence of amorphous or graphitic carbon. All remaining materials are due to metal salts and oxides.

Black mass from the NMC batteries with a high SoC contained about 2 wt% solvents, about 10 wt% of plastic like components and about 36 wt% of amorphous carbon and graphite, see Table 7. About half of the mass (52 wt%) is due to remaining metal salts and oxides. The NMC batteries with a low SoC resulted in a strikingly similar profile of component distribution (~2 wt% electrolyte solvents, 12 wt%

polymers. ~37 wt% amorphous carbon and graphite and 48 wt% metal salts and oxides). This indicates that the SoC does not have a large influence on carbon containing material composition in the black mass. From a separate casing of one of the NMC batteries, TGA-GC-MS analysis was performed to identify which polymers/materials are in the casing. It was found that a large part of the casing consisted of nylon (PA6), glass fibre, a polymer containing styrene (like ABS) and the printed circuit board (PCB) that is connected to the battery cells consists of a brominated epoxy resin. To study the polymeric content of the black mass from NMC batteries with high SoC, TGA analysis coupled with GC-MS was performed to identify different polymers semi-quantitatively. It was found that in the black mass, small amounts of brominated epoxy resin were found, indicating that part of the shredded PCB ends up in the black mass. In addition, nylon (PA6) was detected (~5-10 wt%) as well as the binder PVDF (~1 wt%).

Table 7: Results of the TGA analysis of the black mass fraction of various trials and the quantification of various type of components.

Black mass fraction	RT~250 °C SVOC (wt%)	~250-~800 °C Polymers (wt%)	> 800 °C Amorphous carbon and graphite (wt%)	Remaining Metal salts and oxides (wt%)
NMC low SoC	2	12	37	48
NMC high SoC	2	10	36	52
NCA high SoC	1-2	4-5	43-44	50
NCA low SoC	1-2	4-5	42-44	50-52
LFP low SoC	4-6	3-4	28-30	61-62
LFP high	4-5	3-4	28-29	64

Next, to compare the black mass from the trials with and without casing, the TGA (coupled with GC-MS) of the black mass from the NCA trials and LFP trials was also analysed, see Table 7. Comparable to NMC, the TGA profiles of the black mass fractions of the NCA and LFP trials of the batteries with a high and low SoC were highly similar, indicating that the SoC has little effect on the carbon containing composition of the black mass. The black mass from the NCA contains 1-2 wt% SVOC, 4-5 wt% polymers, 42-44 wt% amorphous carbon and graphite and 50-52 wt% of metal salts and oxides. The black mass from the LFP batteries contained 4-6 wt% electrolyte solvents, 3-4 wt% polymers, 28-30 wt% amorphous carbon and graphite and 61-64 wt% of metal salts and oxides. When these TGA results are compared between the NMC, NCA and LFP black mass fractions, it is noticed that the NMC black mass has a higher polymer content, most likely caused by the plastic battery casing was still present during shredding. In addition, it is noticed that all black mass fractions contain some electrolyte solvents and most strikingly the LFP black mass (~5 wt%). Furthermore, it is shown that a large part of the black mass consists of graphite or amorphous carbon.

The composition of the polymer/binder components were then identified and quantified by TGA-GC-MS for the NCA and LFP black mass. In addition, the electrolyte composition could be semi-quantitatively measured for the LFP black masses, because these contained a higher loading of electrolyte solvents than the NMC and NCA black mass samples. The polymer content was studied and showed that the NCA black mass contained around 0.5 wt% PVDF binder and the LFP black mass contained considerably more with 2-3 wt%. The LFP black mass contained about 1 wt% EC (quantitatively determined) (with a high boiling point) and the remaining electrolyte solvents consisted of EMC, DEC, and DMC (these three solvents were semi-quantitatively measured).

4.6   SEM analysis

To gain a better understanding of the sizes, shapes, textures, and elemental distribution of the various particles within the black mass fraction, SEM analyses were performed. Because of the time-consuming nature of this analysis, it was decided to only study the NMC and LFP black mass fraction and the assumption was made that NCA and NMC would give similar results due to the chemical more similar nature of NMC and NCA.

NMC black mass

The black mass of the NMC batteries with a high SoC were analysed by SEM analysis. On a first overview image of the black mass, it is noticed that many particles around 10 µm in size are present and fewer of up to a few hundred µm. Based on taking images using secondary electrons (SE) and backscattered electrons (BSE) in combination with EDX analysis, the chemical/elemental composition of various particles could be determined. It was observed that many particles that were present (size typically <50 µm) did not contain any metals. EDX analysis of these particles mainly showed the presence of the elements carbon and oxygen, indicating that these particles are graphite particles or polymers/plastics (Figure 15-A+B). In addition, also particles with similar sizes were observed that gave in BSE mode a lot of contrast. This is in indication that in those particles both carbon containing material and metals were present. EDX analysis of these composite materials showed that a particle like this contains carbon and oxygen, but also Ni, Mn and Co and F. This suggests that a particle like this is an agglomerate of different particles of NMC that are held together by a PVDF binder (containing C and F). An example of this is shown in Figure 15-D that has light parts that are NMC (metal containing) particles, which are held together by PVDF binder (black part in between NMC particles).
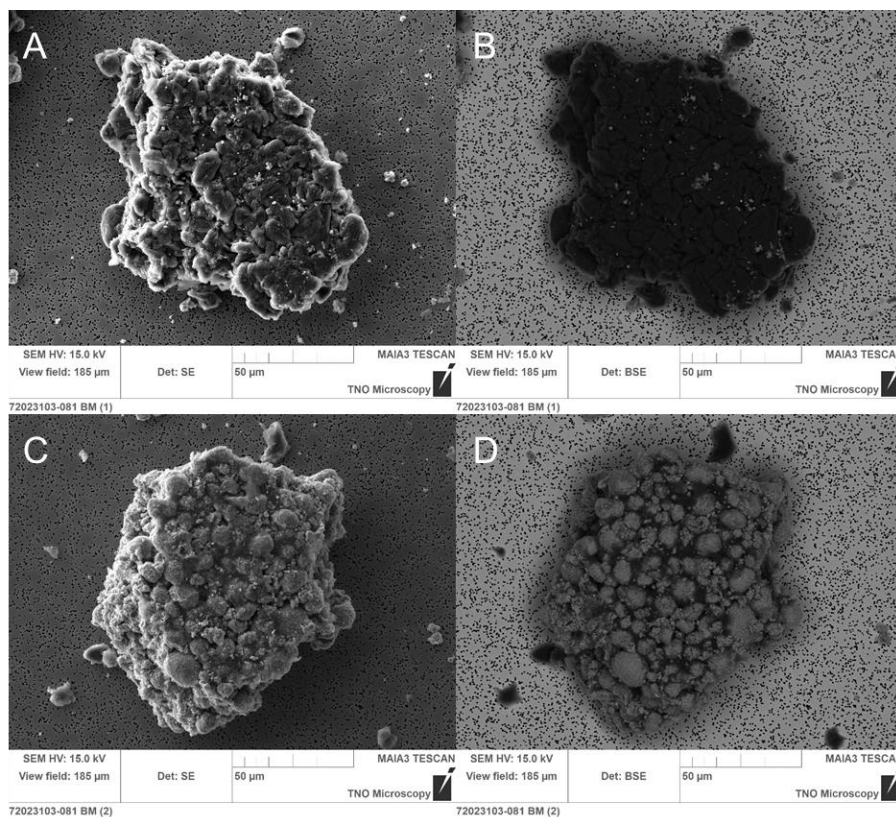

Figure 15: SEM micrographs of the black mass from the NMC trials showing a graphite particle (A + B) and a NMC containing particle (C + D) both taken in two different imaging modes (SE and BSE).

Next to these images, an automatic search method was applied which detects and determines the size and composition of many particles within a sample. Using this method, a size distribution could be determined, which shows what particle sizes are present within the NMC black mass. This analysis showed that around 75% of the particles have a size between 2-10 μm and that about 25% of the particles are between the 10-100 μm, see Figure 16-A. Also, a volume distribution was determined, which showed that about 40% of the cumulative total volume comprises particles in the range of 2-100 μm and that about 50% of the cumulative total volume originates from particles between the 200-300 μm range. An interesting observation was made during the automatic search method when the elemental distribution of the particles was measured using EDX analysis. It showed that in the particle size range 0-30 μm, that about 90% of those particles contained Ni, Mn, and Co (NMC elements). The graphite that is used on the anode of NMC batteries typically are small particles around 20 μm, suggesting that the smallest particles in the black mass are due to the graphite. In all larger particles up to 300 μm the NMC elements are present. This indicates that particles below 30 μm could also be particles other than NMC and that the larger particles originate from the cathode or from the casing (plastics).
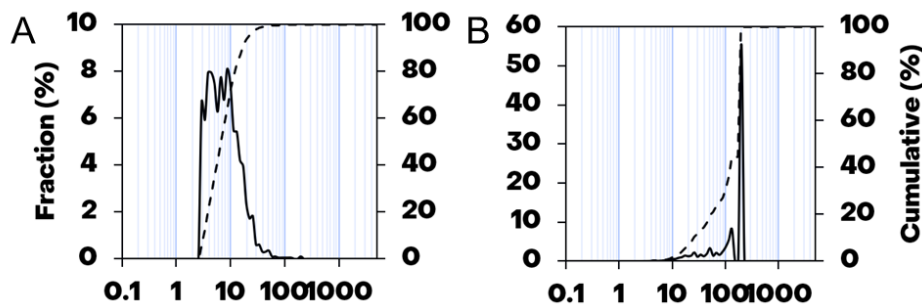

Figure 16: Particle size distribution (μm) of NMC black mass and cumulative number of particles (grey dotted line) (A) and volume distribution over particle size (μm) and total cumulative volume (grey dotted line) over the different particles sizes (μm) (B).

LFP black mass

The black mass obtained from the LFP batteries with a high SoC were analysed with SEM analysis. In an overview of the powdered sample, it was noticed that the particles size of the LFP black mass was clearly smaller than for the NMC particles and by far most of the particles were well below 50 μm in size. Interestingly, when a single particle was zoomed in, it was shown that many of the particles are an agglomerate of many small particles of approximately 1 μm in size, see Figure 17. The SE and BSE images showed that these small crystals contain metals and indeed an EDX analysis of different spots in the agglomerate showed that the crystals are made out of particles of CAM (containing Fe, O, P). Another finding is that also Ni and Co were observed on a few spots, indicating that spillover from a previous battery shredding process has taken place, confirming what was also observed with ICP-MS, as described above.
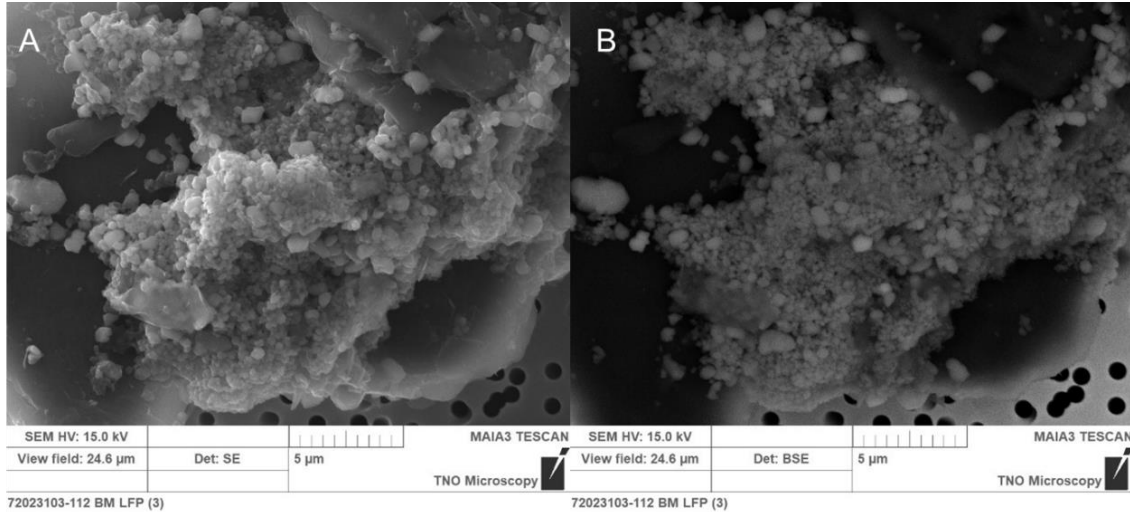
Figure 17: SEM micrograph of a zoom in of an agglomerate of LFP particles in the SE imaging mode (A) and BSE imaging mode, which shows metals at lighter spots (B).

Similar to the NMC SEM analysis, an automatic search method was applied to count the particles, determine their size and elemental composition. Like for NMC, by far most of the particles had a size between 2-10 µm and about 20% of the particles were between 10-40 µm, see Figure 18-A. A difference between the NMC and LFP black mass particles is that the cumulative total volume of particles up to 50 µm is already above 80% (Figure 18-B). This indicates that by far most of the particles are smaller than this size and that the LFP black mass contains on average significantly smaller particles than in the NMC black mass. The distribution of Fe and P over the particles of different sizes was also determined. Up until 30 µm about 95% of the particles contained Fe and P, indicating that these are LFP particles or that the particles also contained some LFP. All analysed particles above 30 µm contain Fe and P, suggesting that these all contain crystals of LFP material. This is similar to the result for NMC black mass particles which also contain graphite up until 30 µm. It could be that this automatic search method for detecting metals overestimates the content of metals for both the NMC and LFP black mass. This is due to the lower sensitivity of carbon and other light elements for EDX analysis of which graphite particles are made of. Therefore, it could be that the number of graphite particles which do not contain cathode active material parts are underestimated.
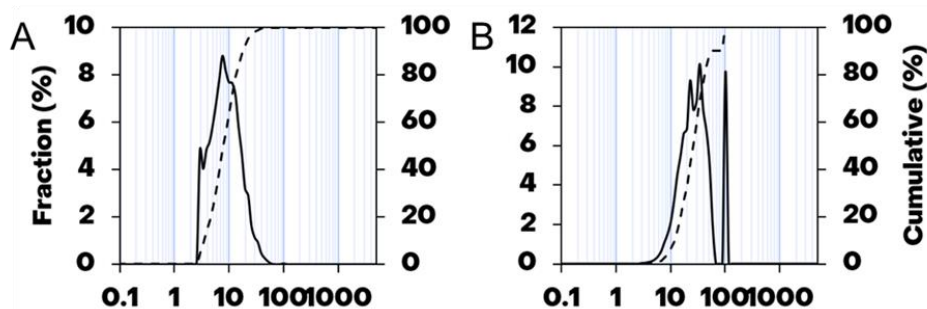

Figure 18: Particle size distribution (µm) of LFP black mass and cumulative number of particles (grey dotted line) (A) and volume distribution over particle size (µm) and total cumulative volume (grey dotted line) over the different particles sizes (µm) (B).

These SEM results of the NMC and LFP black mass showed that the particle sizes are significantly smaller than the sieve size. Typically, during the shredding of battery materials, the copper and aluminium current collectors and other parts of the battery, like the casing and plastic separator, will end

up in more coarse particles. To increase the CAM and graphite content in the black mass fraction and decrease the amount of other materials that end up in the black mass fraction, the sieve size could be optimized. These results show that smaller sieves can be used for the pretreatment process.

5.   Cathode active material recovery from coarse fraction

It is found that in all trials over 50% of the CAM materials was trapped in the coarse fraction (see section 4.4). In order to increase the efficiency of pretreatment process and increase the recovery yield of CAM, additional processing steps were tested to recover more CAM from the coarse fraction. Three experimental procedures were selected for this purpose. The first approach was to treat the coarse fraction with a certain physical agitation like ultrasonic probe or overhead stirrer in aqueous medium. The second approach was to treat coarse fraction with an organic solvent that can dissolve PVDF binders that is most commonly used as a glue to hold cathode and anode films intact and stick them to the current collectors. The third was to sieve the coarse fraction further with and without electrostatic treatment to neutralize any electrostatic interactions that the shredded materials might have and thus to release trapped powders from the coarse fraction.

5.1   Physical agitation of coarse fraction in aqueous medium

Physical agitation was selected as a way to release trapped CAM from the coarse fraction of the shredding trials. This coarse fraction consisted mainly of current collector metal shreddings (aluminium and copper), separator pieces, casing material shreddings (hard plastic, steel, miscellaneous polymeric material) and in this NMC battery trial also pieces of the battery management circuitry. The amount of trapped CAM in this fraction was determined by analysis of the ashed samples as mentioned in the previous chapters of this report.

For all the experiments performed for the recovery of additional CAM, 50 g of the coarse fraction was selected as a representative sample size. Physical agitation sources tested for these experiments were bath sonication, tip sonication and overhead stirrer. First a screening for the recovery efficiencies for these methods was performed. For a 50 g coarse fraction sample from the first trial mixed with 200 mL deionized water bath sonication, tip sonication and overhead stirring gave the recovery yield of 1.14 g, 3.84 g, and 3.80 g of fine powders (black mass) respectively for mixed SoC. Tip sonication and overhead stirring were the most efficient techniques for the recovery of the fine fraction, so these methods were selected to be utilized for the experiments that followed. The appearance of the coarse fraction material before and after recovery process is shown in the images below (Figure 19).

Figure 19: The appearance of coarse fraction material before (left) and after (right) recovery process.

As can be observed from the images, the black residual films on the copper current collectors containing anode active material (graphite) appeared to be mostly removed after the recovery process. However, there were still some pieces of aluminium current collector shreddings containing CAM, that had black residues after the recovery process. This was the first clue that the CAMs were not completely removed from the coarse fraction with the recovery process applied.

After the initial screening, the experiments in aqueous medium with tip sonicator and overhead stirrer were repeated for the coarse fractions of the different trials. The recovery yields of a fine powder fraction per 50 g of coarse fraction from the NMC trials are summarized in the table below.

Table 8: Recovery yields of fine powder of NMC battery coarse fractions with different SoC for physical agitation in aqueous medium.

	NMC Low SoC	NMC High SoC
Tip sonication in water	2.30 g	2.14 g
Overhead stirrer in water	3.04 g	2.26 g

As the recovery yields are the highest using the overhead stirrer, this was the selected procedure for the processing of the NCA battery coarse fractions. In this case the batteries that were shredded did not include the packing material and battery management circuitry, so the coarse fraction obtained had a relatively large portion of current collector shreddings with trapped CAM. This increased the initial yield of recovered material in the trials. However, still about 50% of CAM was trapped in the coarse fraction. The results of the experiments to recover CAM from NCA coarse fractions is summarized in the table below.

Table 9: Recovery yields of fine powder of NCA battery coarse fractions with different SoC for physical agitation in aqueous medium.

	NCA Low SoC	NCA High SoC
Overhead stirrer in water	4.99 g	4.99 g

Even though a significant difference in recovery yields was observed with NMC shreddings for low and high SoC samples (3.04 g vs 2.26 g for Low SoC vs High SoC, respectively, Table 8), not much difference was observed for different SoC NCA samples (see Table 9). The reason for the similar recovery yields for high and low SoC battery shreddings was not clear and can be a subject for further investigation. As mentioned, the material recovery yield was higher for NCA than NMC (for 50 g of processed sample average of 2.65 g for NMC vs. 5 g for NCA). The reason for this observation was the higher ratio of current collectors in the shredded material due to prior removal of casing and battery management system components from the shredded NCA batteries.

5.2   Treatment of coarse fraction with DMSO

Battery active materials are attached to the current collectors through binder polymers like polyvinylidene fluoride (PVDF). Dissolving PVDF to recover CAM using organic solvents was therefore selected as a possible recovery process. Among the organic solvents that can dissolve PVDF (Marshall 2021) DMSO comes forward as a prominent alternative with its high solubilizing ability and its non-toxic nature. For the recovery experiments 200 mL of DMSO was mixed with 50 g of coarse fraction from

NMC and NCA shredding trials using overhead stirrer. The yields for recovered material are summarized in table below:

Table 10: Recovery yields of fine powder for NMC and NCA battery coarse fractions with different SoC with DMSO treatment.

	Low SoC	High SoC
DMSO – NMC	2.05 g	1.59 g
DMSO – NCA	2.33 g	3.38 g

Surprisingly, for both NMC and NCA coarse fraction, the yield obtained by DMSO treatment was not as high as the aqueous medium, even though DMSO was expected to release binder more efficiently than water. This might be an indication of changes of the polymer structures as battery ages or changes in the battery active materials and current collector interface due to cycling or during the exothermic shredding, but a more detailed investigation is needed to clarify these mechanisms.

5.3   Sieving of coarse fraction with and without electrostatic neutralization

Electrostatic interactions within the shredded material was also nominated as a possible reason for the CAM to remain in the coarse fraction. To investigate if this was a prominent force during the separation, recovery experiments were performed with dry sieving with and without prior electrostatic neutralization. For these experiments 50 g of NMC coarse material was sieved with a 2 mm sieve size. For electrostatic neutralization a neutralizer was applied for 30 seconds. The results are summarized in the table below.

Table 11: Recovery yields of fine powder of NMC battery coarse fractions with different SoC using sieving.

	NMC Low SoC	NMC High SoC
Sieving – no pretreatment	0.60 g	0.50 g
Sieving – after electrostatic treatment	0.55 g	0.45 g

The yields of these recovery experiments showed that electrostatic interactions were not a major limiting factor for the separation of black mass. And overall, the recovery yields achieved by dry sieving were much lower compared to water or organic solvent based recovery experiments performed.

5.4   ICP-MS analysis of coarse fraction and recovered black mass

In order to assess the quality of the recovered fine powder/black mass from the coarse fraction of the NMC battery trial, ICP-MS measurements were performed on this solid. Nickel, cobalt, and manganese were the main elements of concern when analysing the results of these measurements since together they are the main components of the CAM and their amount in the black mass determines the economic value of the black mass. The amount of recovered black mass from 50 g coarse fraction together with the CAM content (Li, Ni, Co, and Mn) is given in the table below. For comparison, the CAM content in the original black mass fraction from the NMC trials is added to the table.

Table 12: Recovery yield and CAM content of the fine powder obtained from the 50 g NMC coarse fractions with different SoC from various recovery methods.

	Recovered mass (g)	CAM content (wt%)
Tip sonication in water (NMC low SoC)	2.30 g	22.6
Tip sonication in water (NMC high SoC)	2.14 g	25.6
Overhead stirrer in water (NMC low SoC)	3.04 g	24.2
Overhead stirrer in water (NMC high SoC)	2.26 g	25.3
Overhead stirrer in DMSO (NMC low SoC)	2.05 g	29.8
Overhead stirrer in DMSO (NMC high SoC)	1.59 g	25.2
BM fraction trial 1 (NMC low SoC)	-	26.1
BM fraction trial 2 (NMC high SoC)	-	22.2

The ICP-MS analysis results for the recovered black mass from the coarse fraction show an on average (Table 12) higher metal content than the black mass produced during the trial with high SoC, which is 22.2% (low SoC gave comparable 26.1% of CAM content). The recovered black mass contained 9.9 wt% of Ni, 3.9 wt% of Co, 5.2 wt% of Mn, and 3.2 wt% of Li with a total CAM content of 22.2 wt% (. This shows that the recovered fine powder has a comparable quality compared to the initially collected black mass fraction and some residual material on the aluminium current collectors was successfully recovered besides graphite.

However, there was still remaining CAM on the current collectors. Using the analysis results of the remaining CAM amount at the coarse fraction for NMC battery trials and considering how much black mass was further recovered through the previously presented experiments, it is clear that a large fraction of the CAM remains trapped within the coarse fraction. An overview of the estimated weight distribution for shredding a 1000 g of NMC batteries can be seen in the figure below. Figure 20 gives an average estimation of recovered and trapped CAM after shredding and recovery experiments. Results of detailed analysis of the amount of trapped CAM in the coarse fraction of the various trials after recovery experiments can be further found in the Appendix Table A4.
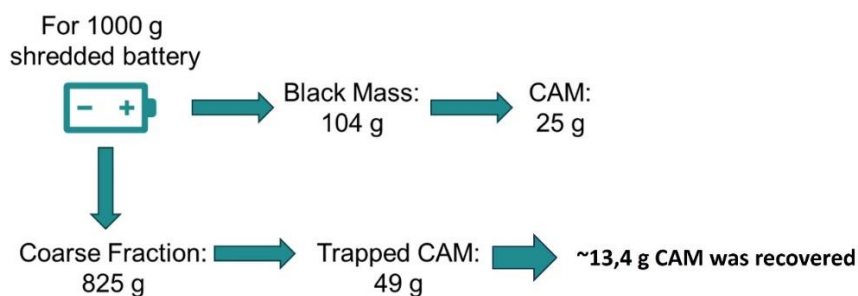

Figure 20: The weight distribution of CAM for a hypothetical 1000 g battery shredding of NMC batteries in casing. 13.4 g CAM per 1000 g of batteries can potentially be recovered from the coarse fraction.

From these results it can be noticed that the conditions for the recovery of the black mass needs to be further optimized and new strategies and processes need to be developed to increase the yields of recovered black mass further. The new battery regulation by European Union, which was put into force on 17 August 2023, dictates recycling targets for cobalt and nickel as 90% and for lithium as 50% by 2028 and these targets further increase to 95% for cobalt and nickel and to 80% for lithium by 2032 (Parliament, 2023). Compared to these targets, the shredding process investigated in this project provided a recovery efficiency of only 34%, which makes it impossible to achieve the EU targets. Even with further recovery experiments, almost 50% of the metals such as cobalt and nickel were still trapped in the coarse fraction. The efficiency of the pre-processing steps needs to be at least over 95% in order to comply with EU targets, since the efficiency of the hydrometallurgical process that follows will also further affect the overall recovery efficiency of metals. Therefore, substantial improvement on the pre-processing step is needed to increase the recovery efficiency of the CAM from lithium ion batteries.

6.   Conclusion and Recommendations

Current pretreatment processes for the recycling of end-of-life lithium ion batteries, yielding black mass as an end product, result in significant losses of the valuable cathode active materials (CAM) that remain in the coarser fractions rather than ending up in the black mass. In addition, these current processes require costly deep discharging process step beforehand to perform comminution of the lithium ion batteries safely. The studied pretreatment technology aims to improve both drawbacks by performing comminution of batteries under inert conditions without the need for deep discharging. This is followed by separation of the liquid and solid fraction by evaporation using a sieving table facilitated by the residual energy from the batteries. Removal of the electrolyte from the solid materials streams also would also enable better separation of black mass from the coarse material fraction. The objective of this work is to assess this pilot-scale pretreatment process (20 kg/h-scale) with an emphasis on studying the efficiency of liquid electrolyte removal and the recovery of CAM in the black mass fraction. This was done by performing several battery shredding trials with varying parameters and collecting and examining all output materials together with analysing the emissions from the pilot scale pretreatment setup.

The efficiency of the electrolyte removal in the pretreatment process was studied by determining the composition of the collected condensate and solid fractions, construction of the mass balances, and studying the process parameters during the shredding trials. The results showed that electrolyte solvents are separated from the solid fractions, but that up to a few percent of the mass of the black mass consist of electrolyte solvents, showing that the separation is not yet completed. The examination of the process during the shredding trials showed that the temperature of the sieving table varied considerably during one trial and had a different average temperature between the various trials. This makes comparison of the electrolyte removal efficiency between the different trials impossible. It was observed that the average temperature of the sieving table was below the boiling points of some of the identified electrolyte solvents (e.g., EMC, DEC, and EC). Nonetheless, examination of the resulting solid fractions showed that most of the electrolyte was removed from the shredded NMC and NCA batteries, but significant amount of electrolyte remains in the solid output streams of the LFP batteries, which can be explained by the much larger cells used in the LFP trials and by a different composition of the electrolyte solvent containing on average more higher boiling solvents. It was shown that it is important to remove all electrolyte from the solid fractions as this has a significant impact on the CAM recovery: electrolyte removal in the LFP trials had been rather inefficient, resulting in a smaller quantity of black mass/CAM separated from the coarse fraction. Therefore, optimization of this part of the setup to control the temperature of the sieving table and increase the length of the sieving table or increase the residence time in the sieving table to allow full evaporation of the electrolyte solvents could result in higher CAM recovery. In addition, it could be beneficial to add more extraction points to allow the vapours to pass the condenser more efficiently, and to increase the flow rate of the inert gas used in the process. It was found that the activated carbon filters placed after the condenser have a larger weight gain then the collected electrolyte solvents, indicating that the condensation of the vapours is not optimal at the moment.

The mass balance of the three different battery chemistry trials were based on 20 kg-scale trials averaged between high and low State of Charge (SoC) for each battery chemistry. The mass balances showed that for all trials more than 97% of the mass could be accounted for: 98% for the NMC trials, 97% for the NCA trials and 98% for the LFP trials, indicating that most of the mass is recovered. This translates to about 300-400 g loss in mass for the NMC, NCA and LFP trials. The monitoring and collection of emissions from the setup during shredding trials resulted in an estimation of the release of

volatile organic compounds and particulate matter. The measured emissions did not have a significant contribution to the mass balance. It was observed by using the Karl Fischer titration method that the condensates of the various trials contained water. In addition, the CO_2 percentage in the setup's atmosphere was high during the shredding trials. This data indicates that material is burned and/or decomposed in the shredding process with release of gases that are not captured, which can explain (a part of) the mass loss.

Using the mass balance, the black mass recovery was studied in more detail by (elemental) analysis of the solid output fractions. It was found that the CAM content in the black mass was 24% for the NMC trials, 25% for the NCA trials and 25% for the LFP trials when the high and low SoC trial results were averaged. The results also showed that a significant amount of the CAM does not end up in the black mass fraction, but in the coarse fraction: 66% of the CAM ends up in the coarse fraction for the NMC trials and this is 53% for the NCA trials and 85% for the LFP trials. This could be due to the presence of some liquid in the solid fractions that sticks fine powders to the coarse material. Therefore, methods that enable a better removal of the electrolyte solvents from the solid fractions should be investigated. In addition, the effect of a more effective vibration/shaking of the sieving table and proper choice of the used sieve(s) on the separation of black mass from the coarse fraction should be investigated. Analysis of the black mass fraction showed that CAM in the black mass has a significant smaller particle size than the currently used sieve. This indicates that the choice of sieve diameter could influence the separation efficiency and enable the isolation of black mass with less impurities from coarser aluminium, copper, steel, or plastic particles.

The composition of the (solid) output materials was studied using various chemical analysis methods. This showed that the black mass fraction did not only consist of CAM, and graphite (the fine materials), but also consists of plastics, aluminium and copper current collectors, steel, and some solvents residues. This indicates that the black mass fraction is a complex mixture of materials and that also coarser particles, such as plastics, end up in the fine black mass fraction with the current pretreatment process.

The impact of changing the SoC of the batteries and the presence of battery casing was studied by chemical analysis of the condensate, black mass, and coarse fractions. Based on ICP-MS analysis, it was found that the output materials from the studied individual trials were contaminated by previous shredding trials due to spillover, which makes accurate comparison challenging. In addition, large and significant deviations in the composition of the output materials between the various trials with either low or high SoC were not identified. The influence of the presence of battery casing on the output materials was not found to be significant with the trials that have been performed. Further trials with batteries with the same battery chemistry with and without battery casing could elucidate the influence of the battery casing on the output materials.

Methods to increase the CAM recovery from the coarse fraction were investigated, because it was found from literature that a significant amount of CAM is not accounted for. Out of the tested methods, stirring the coarse fraction in water was found to be the most effective to remove some of the CAM from the coarse fraction. However, most of the CAM remains in the coarse fraction after treatment. This indicates that liberation of CAM from the electrode foils must be optimized to enable increased recovery of CAM from the coarse fraction, to meet the recovery requirement as stipulated the EU Battery Regulation.

Overall, the pretreatment process performs shredding of batteries without prior deep discharging under inert atmosphere. The process separates electrolyte, black mass containing cathode active

materials, and a residual coarse fraction with high amounts of plastics, steel cell casing, current collectors and some of the cathode and anode active materials. The process is shown to be capable of shredding batteries without the need of prior deep discharging and dismantling. However, the separation of the different fractions is not optimal yet as all materials are in some extend mixed up in the various output streams.

7.   References

Diekmann, J., Hanisch, C., Froböse, L., Schälicke, G., Loellhoeffel, T., Fölster, A.-S., & Kwade, A. (2017). Ecological Recycling of Lithium-Ion Batteries from Electric Vehicles with Focus on Mechanical Processes. *Journal of The Electrochemical Society*, *164*(1), A6184. https://doi.org/10.1149/2.0271701jes

Fernandes, Y., Bry, A., & de Persis, S. (2019). Thermal degradation analyses of carbonate solvents used in Li-ion batteries. *Journal of Power Sources*, *414*, 250-251. https://doi.org/10.1016/j.jpowsour.2018.12.077

Kim, S., Bang, J., Yoo, J., Shin, Y., Bae, J., Jeong, J., Kim, K., Dong, P., & Kwon, K. (2021). A comprehensive review on the pretreatment process in lithium-ion battery recycling. *Journal of Cleaner Production*, *294*, 126329. https://doi.org/https://doi.org/10.1016/j.jclepro.2021.126329

Li, J., Ye, H., Wei, J., Yang, B., Gao, S., & He, K. (2023). Capture and migration of particulate matter in activated carbon sintering flue gas purification system based on ultra-low emission target. *Fuel*, *350*, 128764. https://doi.org/10.1016/j.fuel.2023.128764

Latini, D., Vaccari, M., Lagnoni, M., Orefice, M., Mathieux, F., Huisman, J., Tognotti, L., & Bertei, A. (2022). A comprehensive review and classification of unit operations with assessment of outputs quality in lithium-ion battery recycling. *Journal of Power Sources*, *546*, 231979. https://doi.org/https://doi.org/10.1016/j.jpowsour.2022.231979

Marshall, J. E., Zhenova, A., Roberts, S., Petchey, T., Zhu, P., Dancer, C. E. J., McElroy, C. R., Kendrick, E., & Goodship, V. (2021). On the Solubility and Stability of Polyvinylidene Fluoride. *Polymers*, *13*(9), 1354. https://doi.org/10.3390/polym13091354

REGULATION OF THE EUROPEAN PARLIAMENT AND OF THE COUNCIL concerning batteries and waste batteries, amending Directive 2008/98/EC and Regulation (EU) 2019/1020 and repealing Directive 2006/66/EC, (2023).

8.   Appendices

A. Mass balances

Table A1: Mass balance of NMC battery cell trials.

Input (g)		Output (g)		
Battery cells	25 078.5	Black mass fraction		2 608.0
		Coarse fraction		20 689.0
		Liquid fraction		587.0
		*Condensate**	*177.0*	
		In AC filters	*410.0*	
		Extra solid fraction		784.0
Total	25 078.5			24 668.0
Delta				410.5

* An estimated additional 30-40 g of condensate was spilled during collection.

Table A2: Mass balance of NCA battery cell trials.

Input (g)		Output (g)		
Battery cells	14 883.0	Black mass fraction		5 404.0
		Coarse fraction		8 171.5
		Liquid fraction		881.0
		Condensate	*323.5*	
		In AC filters	*557.5*	
Total	14 883.0			14 456.5
Delta				426.5

Table A3: Mass balance of LFP battery cell trials.

	Input (g)		Output (g)	
	Battery cells	19 751.0	Black mass fraction	1 950.5
			Coarse fraction	14 713.5
			Liquid fraction	1015.0
			Condensate	*575.5*
			In AC filters	*439.5*
			Extra solid fraction	1 736.0
Total		19 751.0		19 415.0
Delta				336.0

B. ICP-MS analysis

For the ICP-MS analysis, both a microwave destruction method and an open destruction method were used to dissolve the metal content of the black mass samples of the high charge batteries. Independent of the destruction method, highly similar results were obtained, indicating that the simpler open destruction method is sufficient for reliable results.

Representative samples of black mass were taken for ICP-MS analysis and all different products analysed were measured in duplo or quadruplo. The following elements were quantified: Li, Ni, Mn, Co, P, Al, Cu, Fe, Zn, Sn, Cr, Sn, Pb. The results of the ICP-MS analysis of the black mass and of the ashed coarse fraction of the different trials are shown in Table A4. It can be noticed from the data that some elements, like Fe, Al or Cu have a larger standard deviation than for the CAM elements, which is due to the larger grain size of the particles of these elements and the larger inhomogeneity of those in the sample compared to the fine sized particles of the CAM elements.

Table A4: ICP-MS analysis results of the black mass and (ashed) coarse fractions of the different trials in wt% with the standard deviation in brackets.

	Co (wt%)	Mn (wt%)	Ni (wt%)	Li (wt%)	Al (wt%)	Cu (wt%)	Fe (wt%)	P (wt%)
BM high charge NMC	3.9 (0.2)	5.2 (0.3)	9.9 (0.5)	3.2 (0.2)	2.5 (0.4)	3.3 (1.4)	1.3 (2.2)	0.6 (0.4)
Coarse high charge NMC	0.9 (0.03)	1.0 (0.02)	2.5 (0.08)	0.3 (0.1)	0.7 (0.08)	4.1 (0.3)	0.4 (0.05)	1.0 (0.02)
BM recovered overhead stirrer high charge	0.5 (0.04)	0.6 (0.03)	1.3 (0.09)	0.1 (0.01)	0.7 (0.1)	3.1 (0.2)	0.2 (0.01)	1.1 (0.03)
BM recovered tip sonicator high charge	0.7 (0.07)	0.9 (0.08)	2.0 (0.2)	0.2 (0.0)	1.1 (0.06)	3.2 (0.2)	0.3 (0.0)	1.3 (0.01)
BM low charge NMC	4.6 (0.3)	6.2 (0.6)	12.0 (1.1)	3.3 (0.2)	2.6 (0.7)	4.5 (0.7)	0.6 (0.2)	0.8 (0.08)
Coarse low charge NMC	1.4 (0.01)	1.5 (0.01)	3.7 (0.04)	0.7 (0.01)	1.1 (0.2)	6.5 (0.1)	0.3 (0.06)	1.1 (0.03)
BM recovered overhead stirrer DMSO low charge	0.9 (0.03)	1.1 (0.01)	2.6 (0.05)	0.4 (0.01)	1.2 (0.02)	4.8 (0.08)	0.2 (0.0)	1.1 (0.08)
BM recovered overhead stirrer low charge	0.9 (0.01)	1.1 (0.01)	2.5 (0.04)	0.3 (0.01)	1.1 (0.2)	5.7 (0.3)	0.4 (0.04)	1.1 (0.02)
BM high charge NCA	2.9 (0.1)	0.1 (0.01)	16.2 (0.6)	3.2 (0.03)	1.4 (0.03)	1.4 (0.2)	3.7 (0.7)	2.4 (0.3)
Coarse high charge NCA	2.4 (0.1)	0 (0)	13.3 (0.7)	1.6 (0.02)	4.0 (0.2)	8.8 (0.9)	1.1 (0.07)	0.6 (0.04)
BM low charge NCA	3.7 (0.1)	0 (0.01)	20.6 (0.3)	3.4 (0.07)	0.9 (0.1)	0.9 (0.3)	0.9 (0.06)	1.0 (0.09)
Coarse low charge NCA	2.9 (0.1)	0 (0)	15.7 (0.7)	1.9 (0.06)	5.6 (0.4)	10.9 (0.7)	0.8 (0.1)	0.3 (0.04)
BM high charge LFP	0.2 (0.06)	0.06 (0.0)	0.9 (0.3)	2.4 (0.04)	3.5 (0.5)	3.4 (0.7)	16.4 (0.2)	9.1 (0.2)
Coarse high charge LFP	0.1 (0.0)	0 (0)	0.3 (0.02)	1.5 (0.02)	4.4 (1.3)	5.8 (0.6)	10.8 (0.01)	5.9 (0.15)
BM low charge LFP	0.9 (0.09)	0.09 (0.0)	5.1 (0.5)	2.5 (0.03)	2.8 (0.4)	3.7 (1.1)	12.2 (0.8)	7.3 (0.4)
Coarse low charge LFP	0.2 (0.01)	0.01 (0.0)	1.0 (0.03)	1.8 (0.04)	3.1 (0.02)	7.4 (0.4)	12.2 (0.4)	6.8 (0.2)

C. Results from SEM analyses

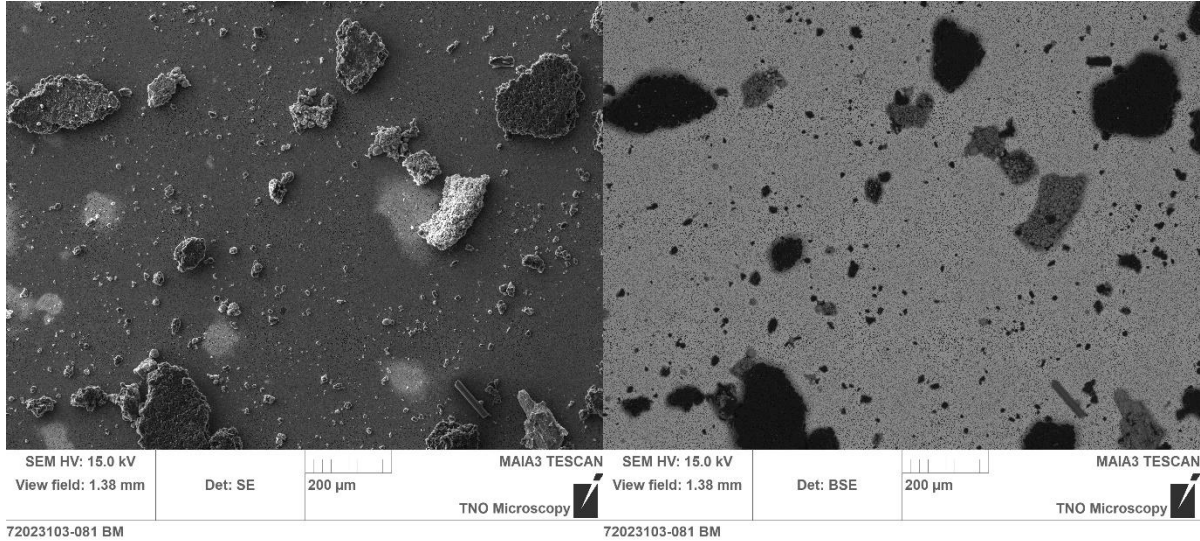Black mass: NMC high charge fraction

Figure A1: SEM images at 200x magnification of black mass from the NMC high charge trial in two different scanning modes.
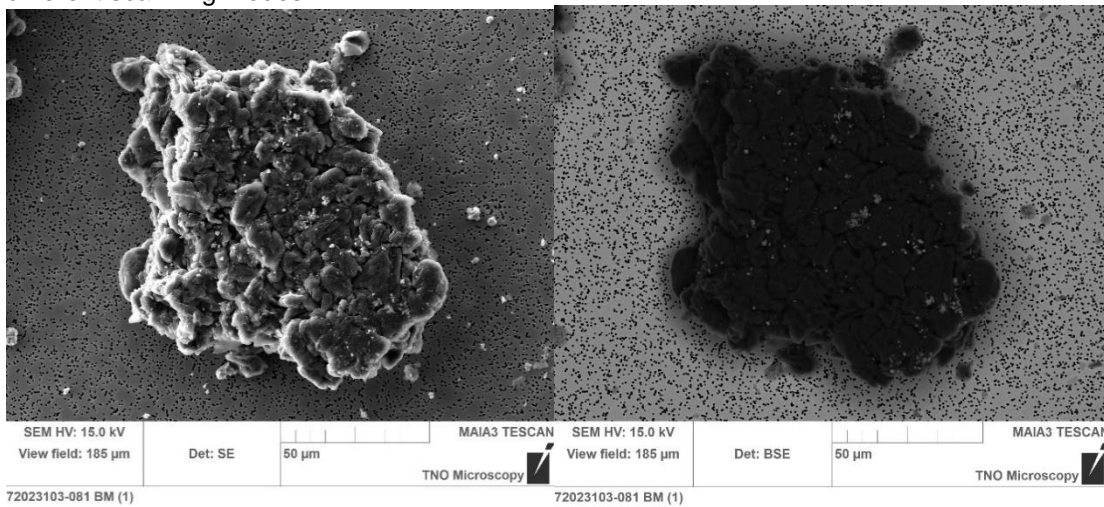

Figure A2: SEM images of a black mass particle from the NMC high charge trial in two different scanning modes. The BSE mode indicates that this a graphite particle.
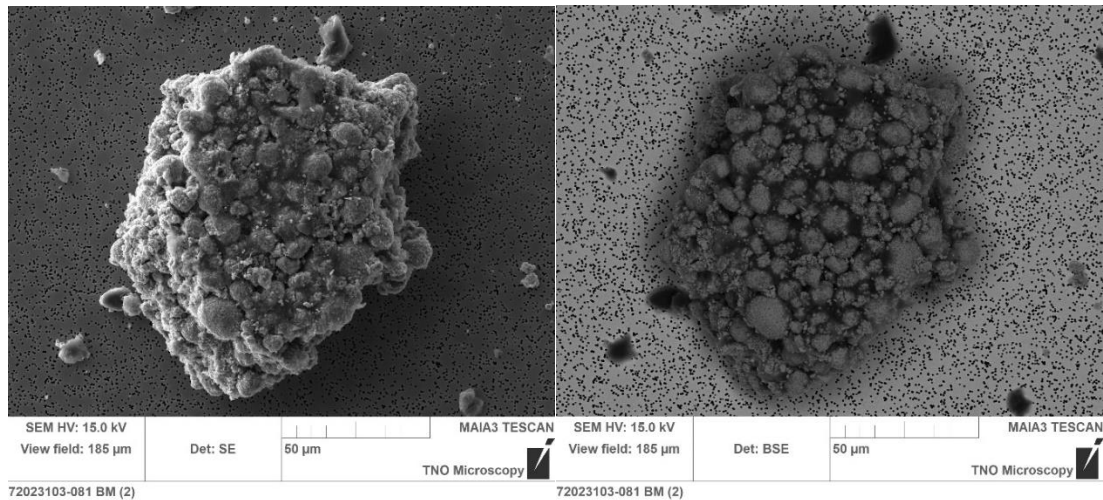
Figure A3: SEM images of a black mass particle from the NMC high charge trial in two different scanning modes. The BSE mode indicates that this a NMC particle hold together by organic binder due to the grey and black contrast.
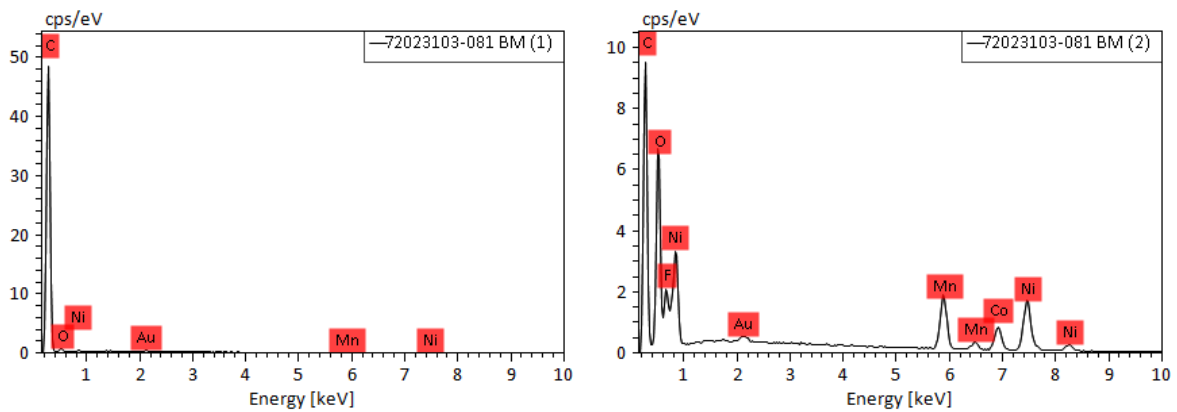
Figure A4: EDX analysis of two different black mass particles of high charge NMC, of which one suggests that it is a graphite particle (left, due to the elements present) and the other an image of an NMC particle (right, due to the elements present).

Black mass: LFP high charge fraction
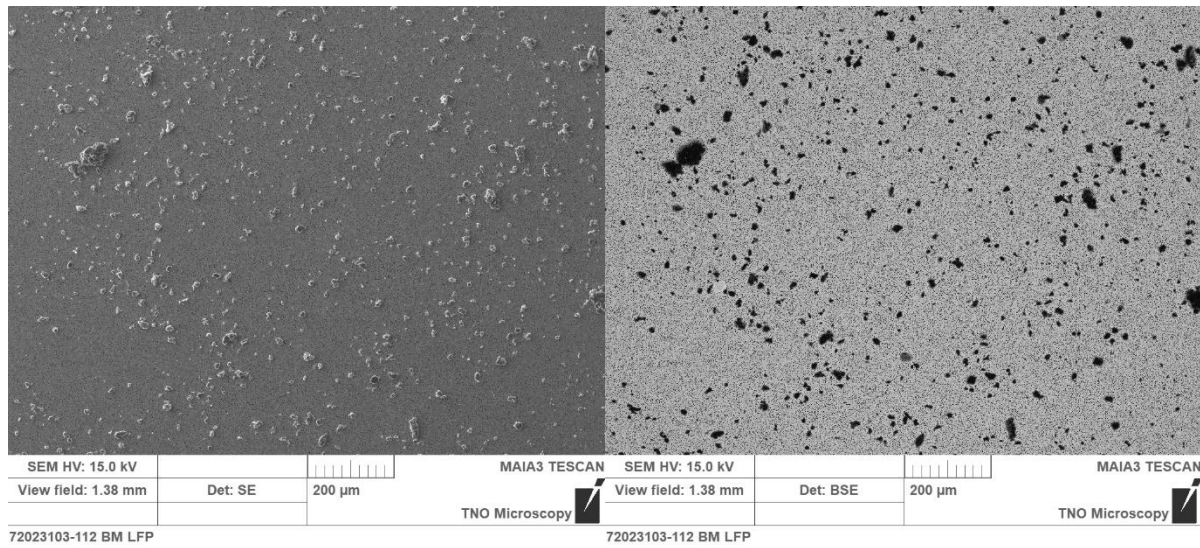
Figure A5: SEM images at 200x magnification of black mass from the LFP high charge trial in two different scanning modes. It is clearly visible that this sample contains smaller particles than for the NMC black mass (above) or the material collected on the filters (down below).
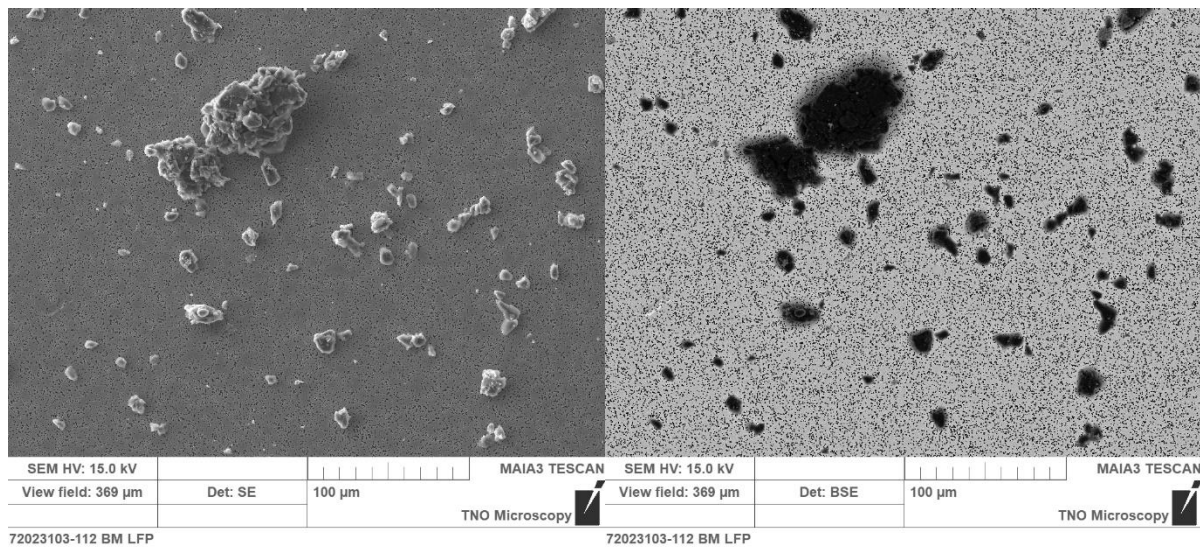
Figure A6: SEM images at 750x magnification of black mass from the LFP high charge trial in two different scanning modes. The BSE mode image shows a contrast of the particles suggesting that these are graphite/organic particles.
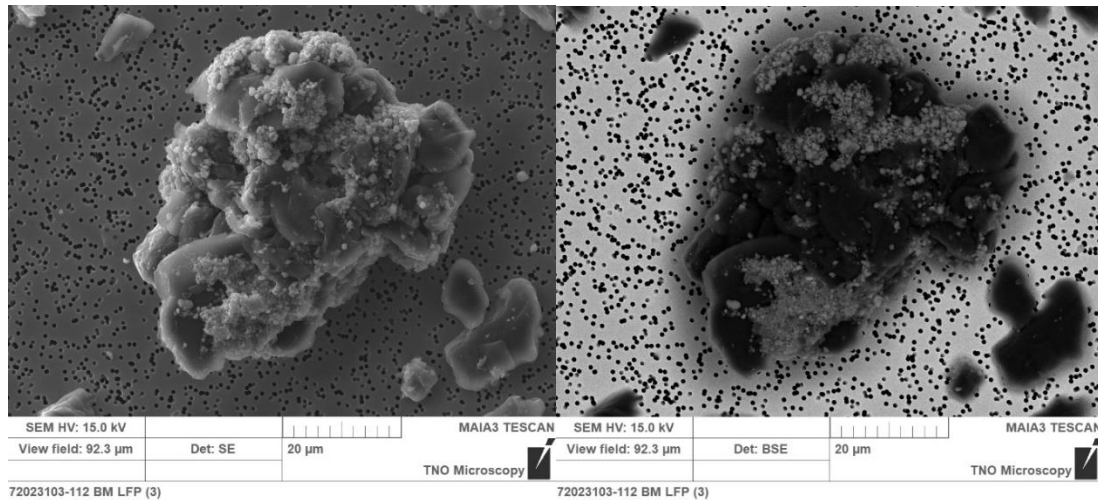
Figure A7: SEM images of an LFP particle from the black mass of the LFP high charge trial in two different scanning modes. The contrast in the BSE mode image suggests that a conglomerate of very small LFP crystals is held together by a binder.
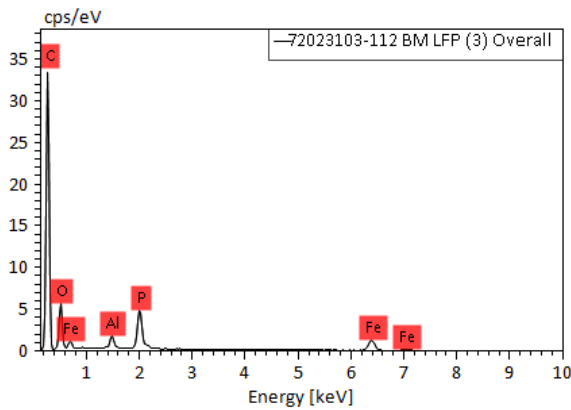
Figure A8: EDX analysis of an LFP particle from the black mass of the LFP high charge trial showing the presence of Fe, P, C, O and Al.
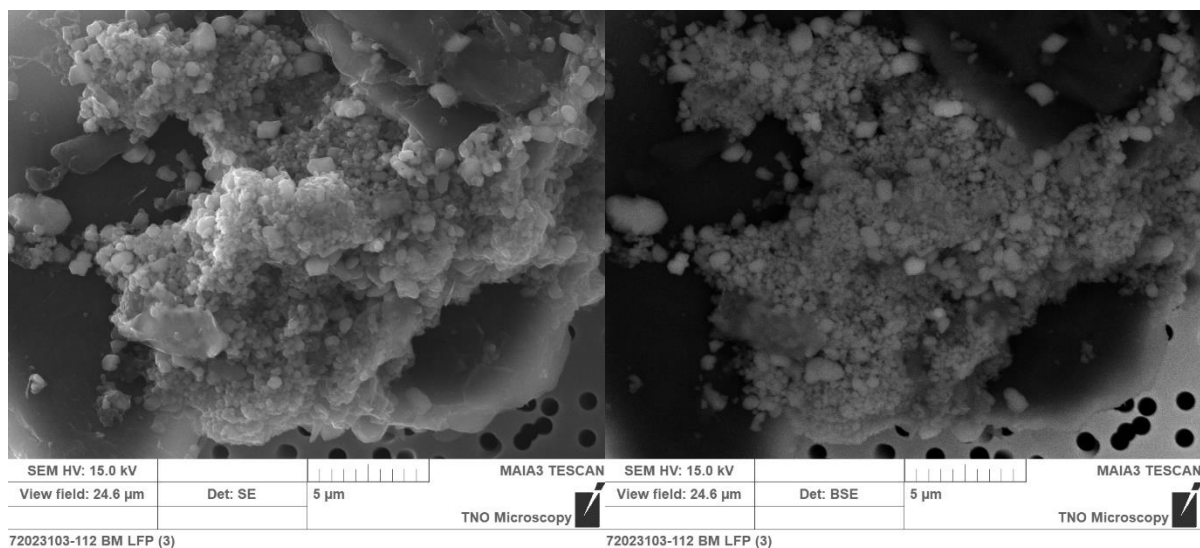
Figure A9: zoom-in SEM images of an LFP particle from the black mass of the LFP high charge trial in two different scanning modes showing the small size of the different LFP particles clustered together.
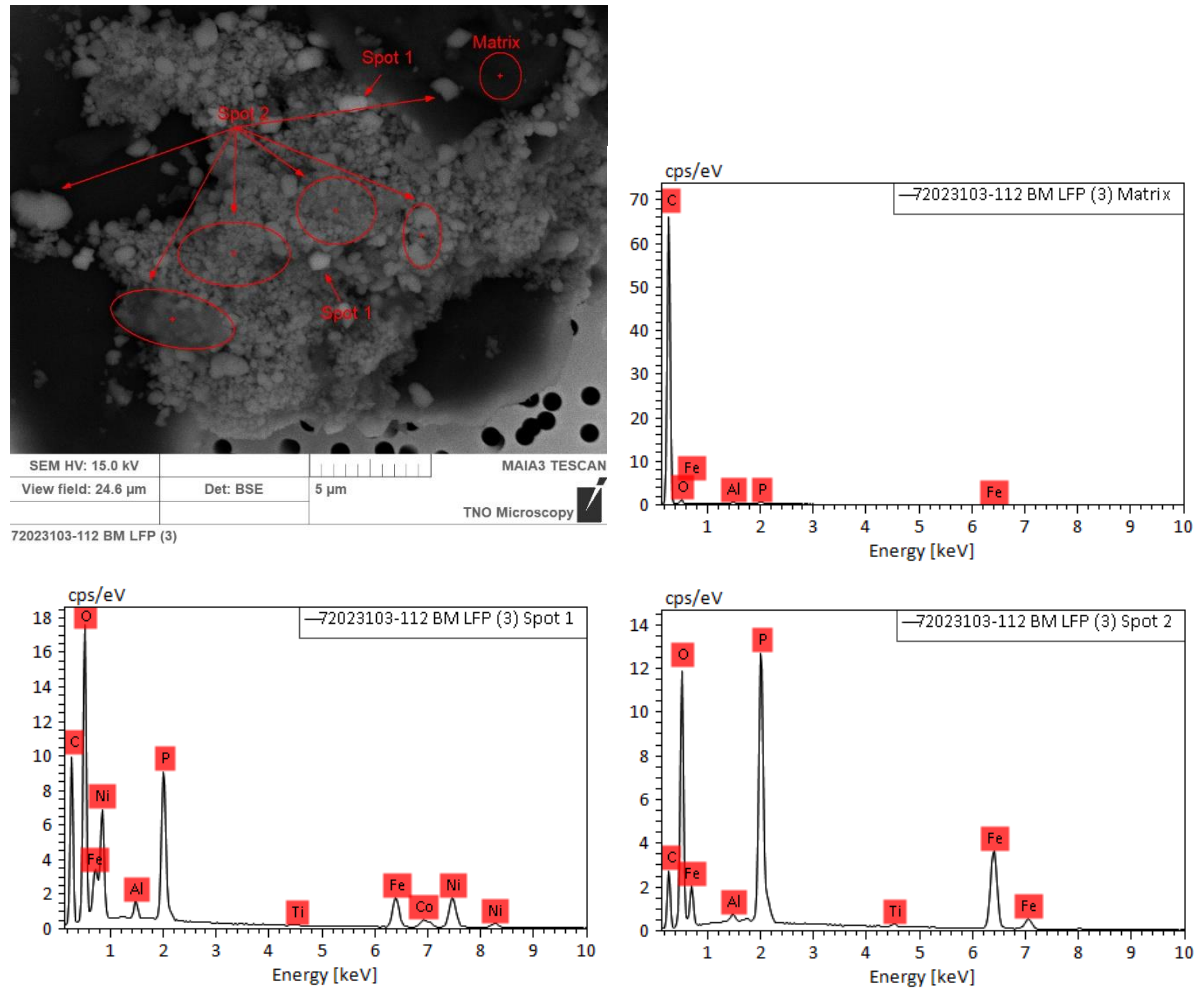
Figure A10: zoom-in SEM images of an LFP particle from the black mass of the LFP high charge trial and the EDX spectrum at different spots, showing the elemental distribution.

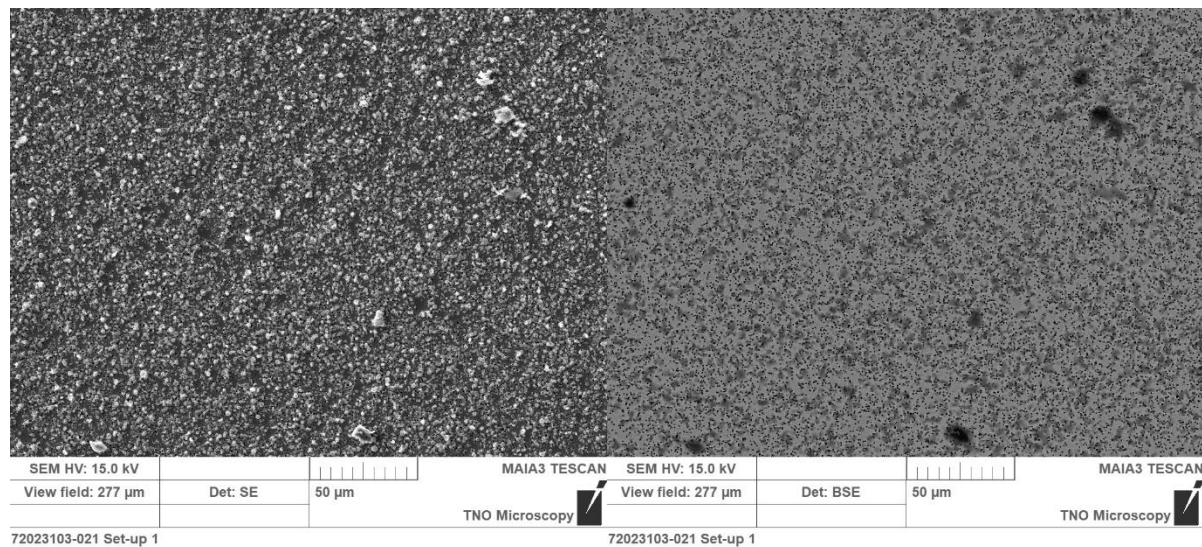## Air sample filters NMC trials

Figure A11: SEM overview image of the air emission filter (magnification: 1kx) of setup 1 showing that only a few particles were collected.
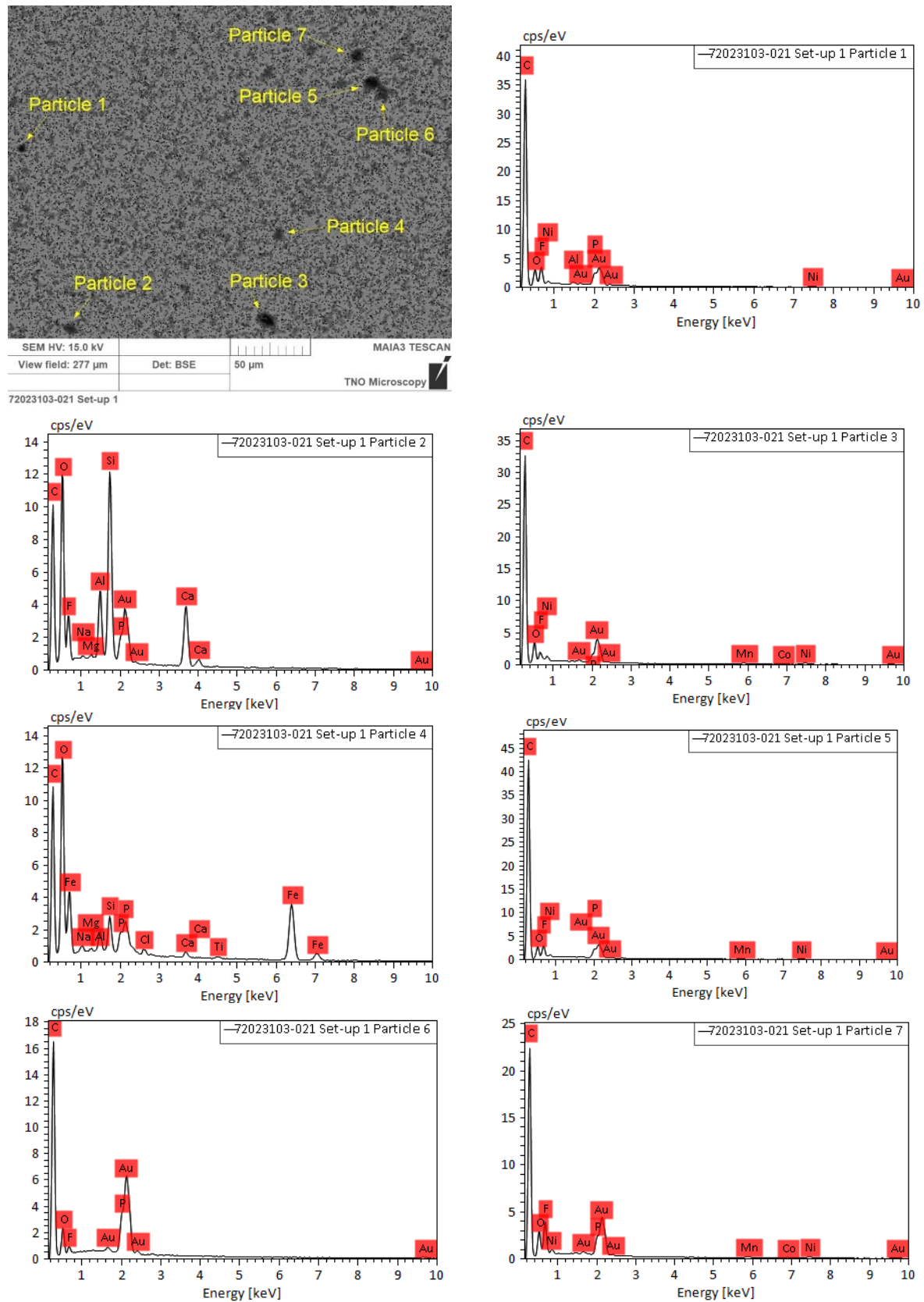
Figure A12: SEM overview image of the air emission filter (magnification: 1kx) of setup 1 and the EDX spectrum with the elemental distribution of various particles observed.
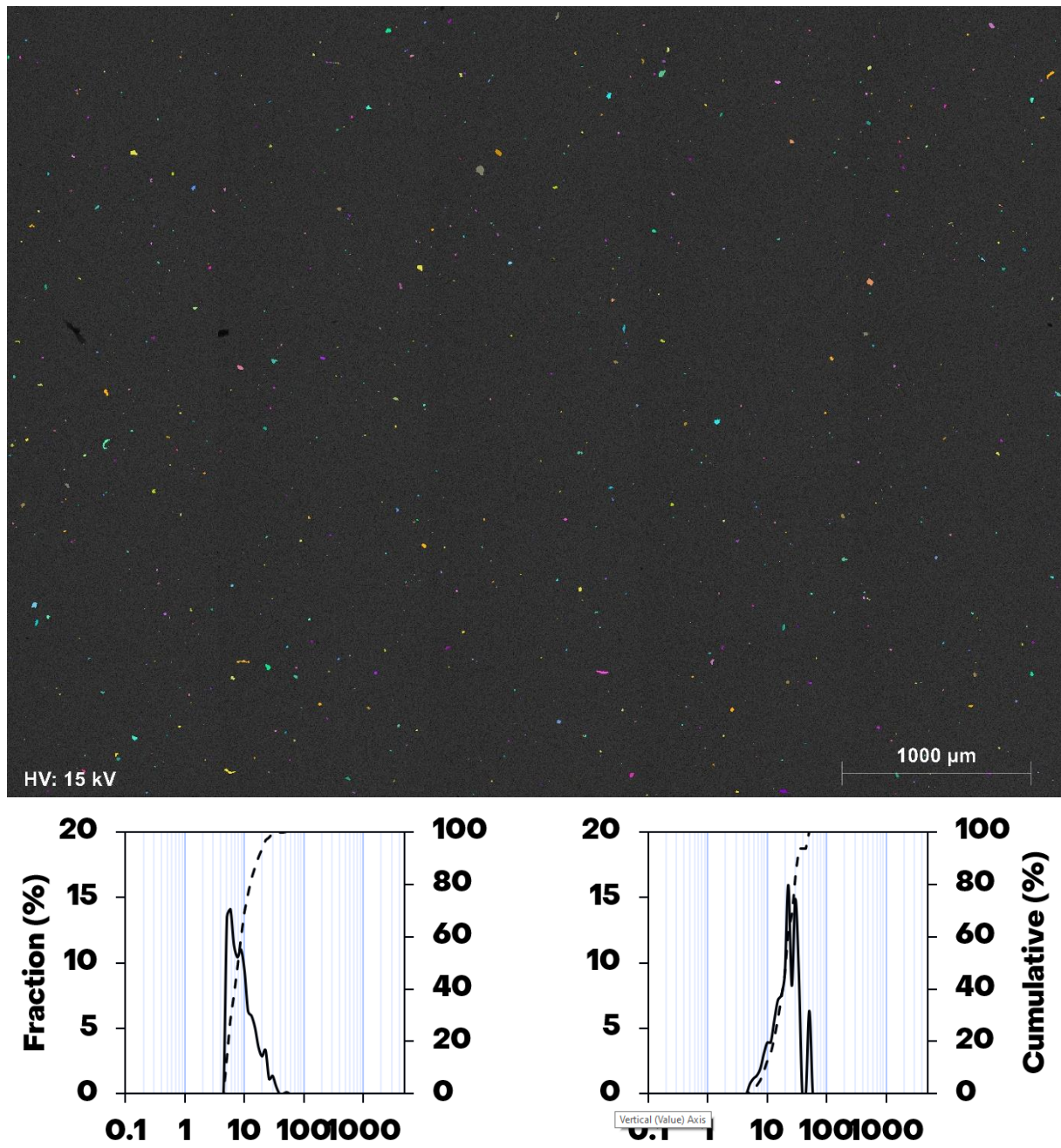
Figure A13: Particle size distribution (µm) of the air emission collected on the gold filter and cumulative number of particles (grey dotted line) (left) and volume distribution over particle size (µm) and total cumulative volume (grey dotted line) over the different particles sizes (µm) (right).
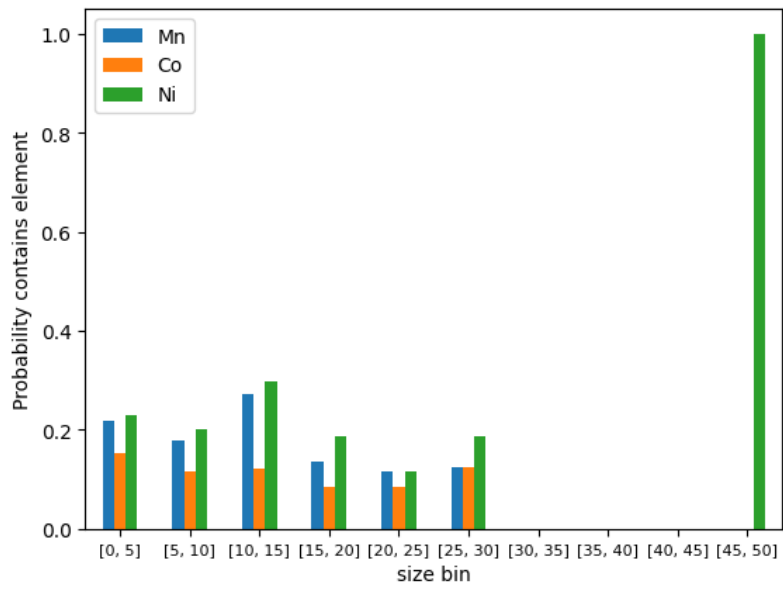
Figure A14: Percentage of particles on collected on the filter of setup 1 containing Ni, Mn, and Co in various size distributions (µm).